INVESTIGATIONS OF COSMIC RADIATION AND OF THE TERRESTRIAL CORPUSCULAR RADIATION BY MEANS OF ROCKETS AND SATELLITES

S. N. VERNOV and A. E. CHUDAKOV

Usp. Fiz. Nauk 70, 585-619 (April, 1960)

THE launching of artificial earth satellites has provided the first possibility of obtaining information on the cosmic space surrounding the earth. The density of the matter at great distances from the earth is so small that, under the prevailing conditions, the total energy of fast particles is found to be comparable with the kinetic energy of the atoms of the medium, the energy of the magnetic field, etc. The properties of the cosmic space are therefore determined by the energy transfer to high-energy particles and vice versa. In contrast, at altitudes of the order of several tens of kilometers, the energy contained in high-energy particles is negligibly small compared with the total energy of motion of all the atoms of the atmosphere. Under these conditions, only solar rays, whose quanta possess very small energy, can influence the state of the atmosphere.

The most interesting result of the measurements carried out in the U.S.S.R. and in the U.S.A. by means of satellites and rockets is the discovery of a new kind of radiation in the vicinity of the earth, consisting of charged particles caught in a trap formed by the magnetic field of the earth. As will be shown below, the intensity of this radiation is so great that it may cause the demagnetization of the earth's magnetic field. The new radiation consists of particles circulating around the earth. It exists only because of the change in the properties of the cosmic space around the earth as a result of the presence of the magnetic field. Because of that, we think it reasonable to call this radiation by the name of terrestrial corpuscular radiation (TCR).

In the present article we report the investigations carried out during the flights of Russian satellites and cosmic rockets.

1. APPARATUS

Gas-discharge and scintillation counters were used by us for the detection of radiation in cosmic space.

The gas-discharge counters measured the total number of electrically-charged particles passing through the counters. The scintillation counter made it possible to carry out an analysis of the radiation. Events with different energies released in a sodium iodide crystal were measured by means of a photomultiplier tube. Thus, it was possible to measure separately the number of x-ray quanta (energy release 40 — 500 kev), of γ rays (energy release of 500 — 5000 kev), and of high-energy particles traversing the crystal (energy release > 5000 kev). The crystal had a cylindrical form of 39 mm diameter and 40 mm height. A relativistic particle traversing the crystal along the diameter releases 20,000 kev inside it. Therefore, recording all events of energy release > 5000 kev, we detect practically all high-energy particles, since an energy release of 5000 kev occurs also in the case where the particle passes through the peripheric regions of the crystal (more accurately, if the path of the relativistic particle is > 10 mm).

Pulses above the threshold values were counted by means of transistorized scalers.

In addition to these data, the same scintillation counter made it possible to measure the total ionization produced in the crystal by all types of radiations. A circuit consisting of a neon lamp and a condenser was used for the measurements of small currents in the photomultiplier. The photomultiplier current charges the condenser, and, when the voltage on it reaches the neon-flashing potential, the condenser is discharged and the voltage on it decreases to the value at which the neon lamp becomes extinguished. As the current through the neon lamp is interrupted, the process of charging the condenser by the photomultiplier current begins anew. The number of neon-lamp flashes per unit time serves as a measure of the current. The use of scalers makes it possible to measure the number of flashes of the neon lamp very simply. The experiments have shown that, in this manner, it is possible to measure currents as small as 10^{-10} amp. The current of one of the intermediate dynodes of the photomultiplier is proportional to the total ionization produced in the crystal. In contrast, the current of the photomultiplier anode is determined only by the ionization produced in the crystal in small discrete amounts. In other words, the size of the anode-current pulses increases with the energy release in the crystal only so long as the latter is less than 2×10^8 ev. Beyond that, saturation takes place. Relativistic particles passing diametrally through the crystal release an amount of energy equal to 2×10^7 ev, which is greater than the saturation value by a factor of ten. Because of this, the contribution of relativistic particles is decreased by approximately ten times in measuring the anode current. Measuring the current of one of the intermediate dynodes and the anode current simultaneously, it is possible to determine which particles have contributed most to the ionization in the crystal.

The electronic circuits, i.e., the amplifiers, scalers, etc., were all transistorized. The counters and photomultipliers were supplied from dry cells.

Circuit diagrams of the main components of the rocket- and satellite-borne apparatus are shown in Figs. 1 and 2.

2. THE OUTER ZONE OF THE TERRESTRIAL CORPUSCULAR RADIATION

The second Soviet artificial earth satellite was equipped with two gas-discharge counters.

Data on the radiation intensity above the territory of the U.S.S.R. at 225 — 700 km altitude were obtained between November 3 and 9, 1957.[1] It was established that a slow rise of the intensity with altitude was observed at intermediate latitudes, corresponding to the decrease in the shadow of the earth and to the maximum momentum of particles deflected by the earth's magnetic field. At the same time, an anomalous increase in the number of particles was detected during several flights of the satellite in an area north to the 60th geographic parallel. An especially strong intensity increase was observed on November 7, 1957.

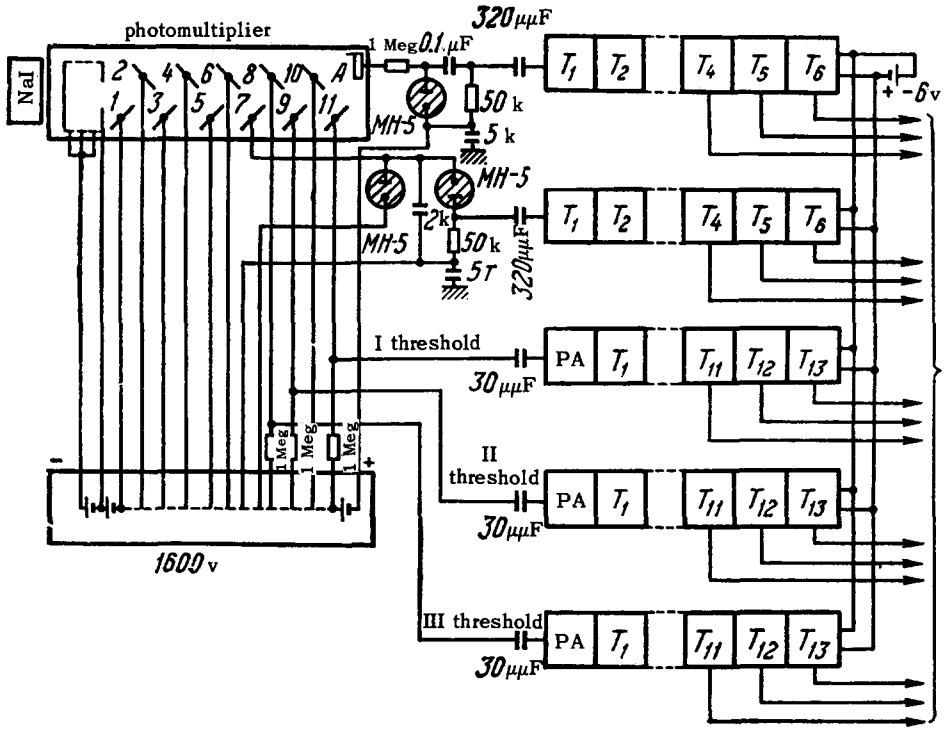

FIG. 1. Block diagram of the scintillation counter. The instrument permits the measurement of the number of pulses with three different energy thresholds, and also the measurement of ionization by recording the mean current of the anode and of the seventh dynode.

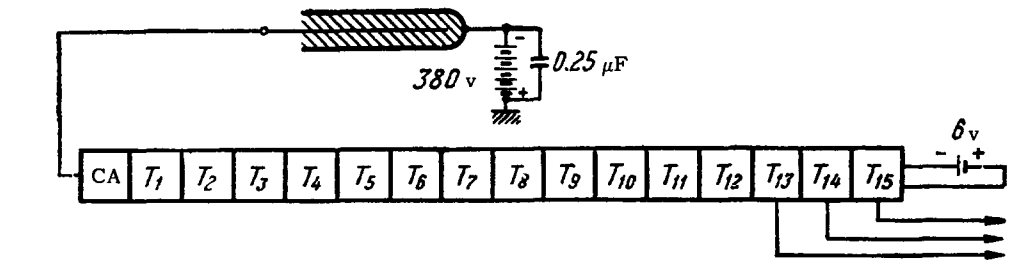

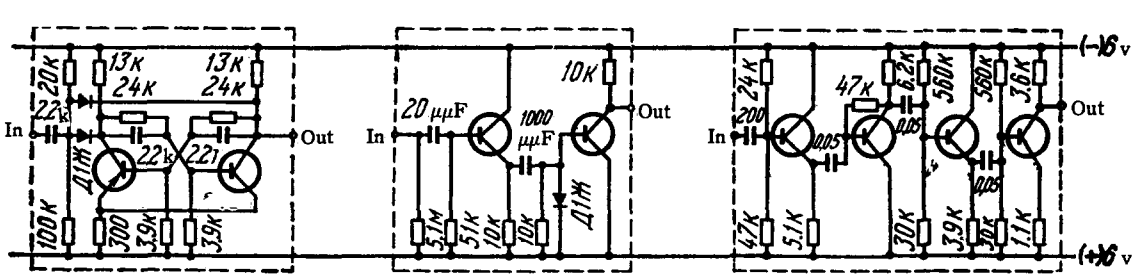

FIG. 2. Block diagram of the gas-discharge counter and basic diagrams of typical circuit elements.

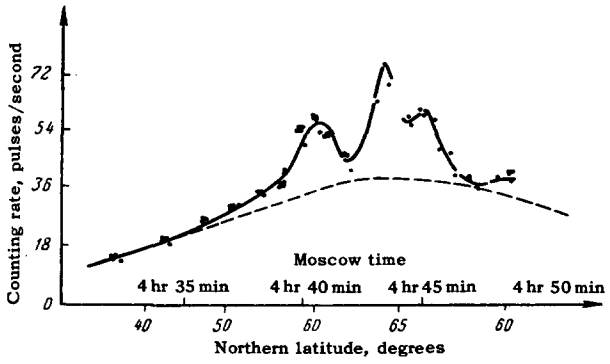

FIG. 3. An example of recordings of the signals of Sputnik II showing an increased intensity at high latitudes on November 7, 1959.

The dashed line represents the usual intensity distribution.

The results of measurements taken between 4 hr 35 min and 4 hr 50 min Moscow time are shown in Fig. 3. The dotted lines denote the average intensity change observed during the other passages of the satellite at the same latitudes. It can be seen from the figure that both instruments, in good agreement with each other, show an increase of more than 50% in the number of particles. The intensity of cosmic radiation at that time remained constant. It is therefore clear that the observed effect indicates the presence of low-energy particles.

The third Soviet artificial earth satellite, launched on May 15, 1958, was equipped with a scintillation counter. The following measurements were carried out by means of this counter: 1) the number of events in which an energy greater than 35 kev was spent in the crystal, 2) the photomultiplier anode current, and 3) the current of one of the intermediate dynodes. It was found that, during each passage through the region where an intensity increase had been observed during the flight of Sputnik II, the counting rate of the scintillation counter (35 kev threshold) increased by a factor of ten or more.

Sample recordings obtained during the flight of Sputnik III in northern latitudes are shown in Fig. 4.

There were cases where only an increase in the counting rate was observed, while the ionization in the crystal remained practically unchanged (Fig. 4a). In other cases (Fig. 4b), an increase in the ionization was also observed together with an increase in the counting rate. From the data on the increase of both ionization and counting rate, it is possible to determine the nature of the detected radiation. It was found that, on the average, the energy loss in the crystal was smaller than 100 kev. This means that the scintillation counter detected x-rays produced as a result of the bombardment of the satellite shell by low-energy electrons.

Thus, as a result of the measurements carried out by means of Sputnik II and Sputnik III, the presence of an external radiation belt around the earth, consisting of a large number of electrons with energy of the order of 100 kev, was first shown.[2] It was also established that this belt is sharply confined to the high-latitude region.

Position of the Outer Zone of TCR with Respect to the Earth

The analysis of the recordings obtained during the flight of Sputnik III made it possible to establish the borders of the outer zone. The coordinates of the satellite's entry into and exit from the northern part of the outer zone are shown in Fig. 5.

As the satellite moved from south to north through a wide range of latitudes, the counting rate of events with energy release greater than 35 kev did not change. However, it increased sharply when the satellite reached the outer zone. As can be seen from Fig. 4, this increase is so sudden that the border of the zone can be established quite exactly. In determining the coordi-

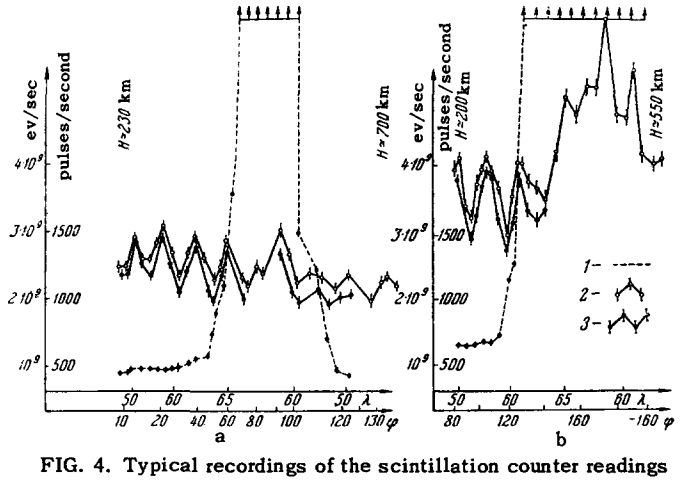

FIG. 4. Typical recordings of the scintillation counter readings at high latitudes over the northern hemisphere.

The x axis represents the latitude λ, longitude φ, and altitude H of the flight of Sputnik III. 1 – counting rate; 2 – ionization in the crystal from dynode-current measurements; 3 – ionization in the crystal from anode-current measurements.

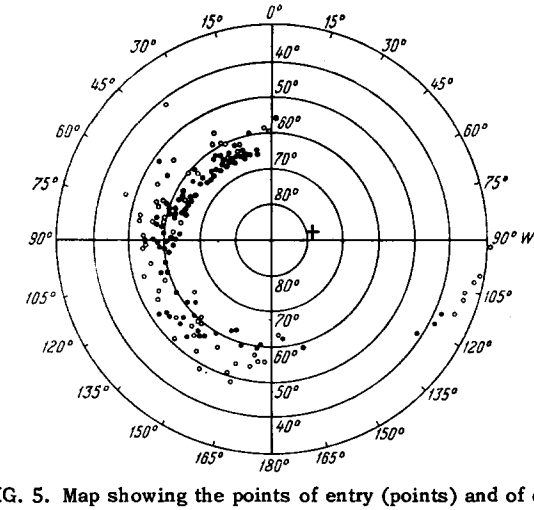

FIG. 5. Map showing the points of entry (points) and of exit (circles) of Sputnik III into and out of the outer zone from the side of low latitudes in the northern hemisphere.

The circles correspond to higher altitudes of the flight. Data refer to the period from May 15 to June 18, 1958. The geomagnetic pole is denoted by the cross.

nates shown in Fig. 5, the place where the counting rate was equal to 1000 pulses per sec was taken as the border of the zone. This value is greater than the intensity outside the zone by almost a factor of two and, therefore, sufficiently well establishes the satellite's presence inside the outer zone. On the other hand, in every one of 300 entries of the satellite into the outer zone, the intensity, without exception, increased by much more than a factor of two.*

The points in Fig. 5 represent the entry coordinates, and the circles the coordinates of exit from the outer zone towards lower latitudes. For the eastern hemisphere, the mean entry point corresponds to the geographic latitude $\lambda = 60.5°$ and an altitude of 270 km, while the mean exit point corresponds to $\lambda = 55.5°$ and an altitude of 600 km. These points are positioned on different lines of force of the magnetic field. The line of force of the magnetic dipole of the earth passing through the point $\lambda = 55.5°$ and $H = 600$ km will, at the altitude of $H = 270$ km, pass through the point with $\lambda = 57°$, where electrons are practically absent. Thus, it can be seen that, along the lines of force of the earth's magnetic field, a steep increase in intensity is observed with increasing distance from the earth. In an analogous way, the line of force passing through the point $\lambda = 60.5°$ and $H = 270$ km will, at an altitude of $H = 600$ km, pass through the point with $\lambda = 59°$, where the intensity is much greater than the 1000 pulses per second measured on the same line of force at an altitude of 270 km.

Electrons of energies as low as 100 kev can move in the magnetic field of the earth only along narrow helices around the lines of force. If the magnetic trap around the earth did not exist, the electron flux could vary only slightly along the magnetic lines of force. However, if the magnetic field forms a trap for the particles, then these execute oscillations from the northern into the southern hemisphere and vice versa. In such a case, one should observe a sharp increase of intensity with increasing distance from the earth along the magnetic line of force (see Sec. 5 of the article). Thus, the data presented above prove that the existence of a high-intensity zone is due to the presence of a magnetic trap in the vicinity of the earth.

In order to follow the variations in the intensity at large distances from the earth, it is necessary to consider first the data obtained during the flight of the third Soviet satellite in the southern hemisphere. Sputnik III flew over the Antartic region at an altitude of about 1800 km. Therefore, a considerably greater ionization increase was observed during the flight of the satellite over the Antarctic than in the northern hemisphere, where its altitude inside the outer zone varied from 300 to 500 km. In the northern part of the outer zone, the ionization increase in the crystal due to the zone radiation amounted to 5×10^8 ev/sec on the average. In the Antarctic, the same quantity was equal to 2×10^{10}ev/sec. Thus, for an altitude increase from 400 to 1800 km, the intensity increased by a factor of 40. The maximum intensity in the outer zone was determined during the flight of the first Soviet cosmic rocket. It was found that the maximum intensity is observed at a distance of about 26,000 km from the center of the earth. At this point, the ionization was equal to 3×10^{11} ev/sec, which is again greater than that found at the altitude of 1800 km, by a factor of 15.

Thus, it can be seen that the intensity increases markedly with increasing distance from the earth along the same line of force. As has been mentioned above, this shows that the electrons are retained in a magnetic trap around the earth.

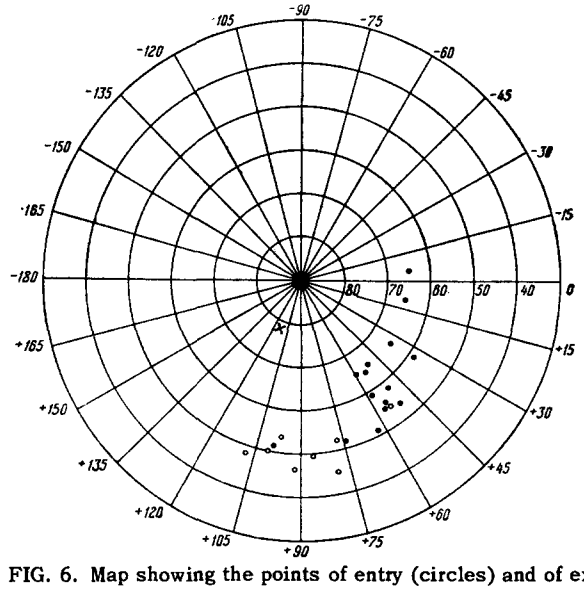

FIG. 6. Map showing the points of entry (circles) and of exit (points) of Sputnik III into and out of the outer zone from the side of high latitudes in the southern hemisphere.

The points correspond to a higher altitude of flight. Data refer to the period from May 20 to June 10, 1958. The geomagnetic pole is denoted by the cross.

In the southern hemisphere, many measurements were taken when the satellite passed near the magnetic pole. It was therefore possible to establish the high-latitude limit of the outer zone. It was established that, at geomagnetic latitudes greater than $65 - 70°$, the electron radiation practically disappears. Results of the measurements in the Antarctic region are shown in Fig. 6.* The points represent the exit coordinates from the zone when the satellite approached the magnetic pole, while the circles represent the entry coordinates when the satellite was going away from the pole.

The distance from the earth over which the outer zone spreads was determined during the flight of the

*The authors are very grateful to all organizations and persons who supplied the recordings of signals of the third Soviet satellite. The recordings sent by Odishaw and Porter from the U.S.A., Elvey from Alaska, Lovell, Davies, and Peterson from England, and Frank, Hertz, and Ogilvy from Australia, were of great interest.

*The authors are grateful to the members of the Antarctic expedition who recorded the signals of Sputnik III.

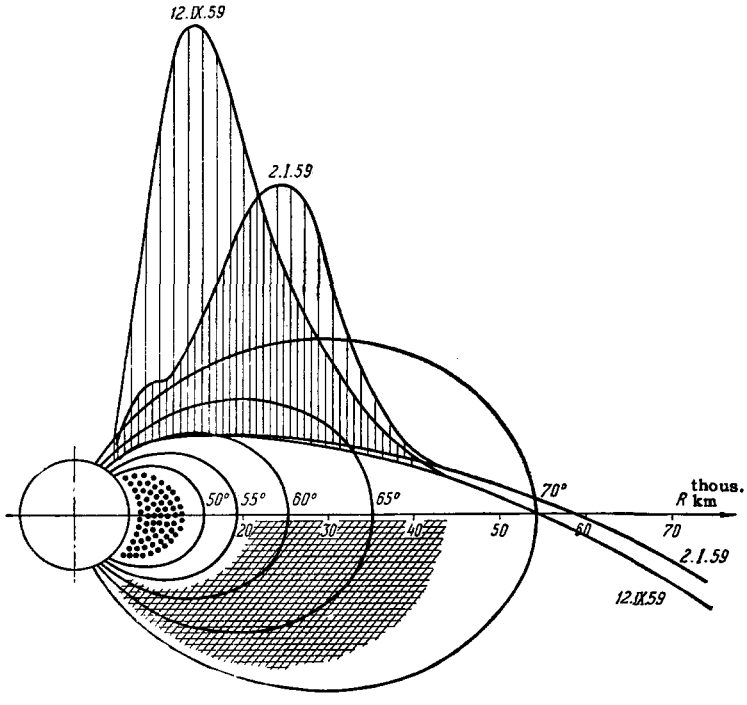

FIG. 7. Trajectories of the first and second cosmic rockets in geomagnetic coordinates.

Vertical lines having the trajectory as their base indicate the intensity at a given point (from the measurement of ionization in the NaI crystal). The magnetic lines of force are labelled according to the geomagnetic latitude at which they intersect the surface of the earth. (The magnetic field is assumed to be a dipole field with coordinates of geomagnetic pole of 78.5° N latitude and 69° W longitude.) The points denote the inner zone, and the crosshatching the outer zone.

first Soviet cosmic rocket.[3] The trajectories of the first and second cosmic rockets, the lines of force of the earth's dipole magnetic field, and the intensity variation along the rocket trajectory, are shown in Fig. 7.

Since the system of coordinates connected with the magnetic dipole of the earth rotates about the earth's axis, the trajectory of the rocket is not a straight line in this coordinate system at great distances from the earth. The numbers near the lines of force indicate the values of the latitudes at which these lines of force intercept the surface of the earth. From Fig. 7 it can be seen that, on January 2, 1959, the maximum radiation intensity was observed at a distance of 26,000 km from the center of the earth. (The intensity is measured in terms of the ionization in the crystal.) At large distances from the earth, the radiation intensity decreases sharply. At a distance of 40,000 km, on the 67° magnetic line of force, the intensity is already 10 times less than the maximum.

Comparing the data on the outward limit of the outer zone obtained in the Antarctic with those obtained during the flight of the first cosmic rocket, it can be seen that, to a first approximation, they correspond with the fact that the lines of force of the magnetic field, at great distances of up to 50,000 km from the earth, are in agreement with the calculated dipole field.

However, as can be seen from Figs. 5 and 6, the borders of the outer zone are different from the geomagnetic parallels near the surface of the earth. The comparison carried out by E. V. Gorchakov shows that the borders of the outer zone coincide with the isochasms, i.e., with the equal-probability lines of occurence of polar aurorae.

It is well known that there are two regions in which polar aurorae are observed fairly often. One is spread out between 60 — 70° geomagnetic latitude, while the second is observed at high latitudes (about 80°). The effective borders of the outer zone correspond, on the average, to the geomagnetic latitudes 55° and 65°. Thus, one of the regions in which polar aurorae are observed partially overlaps the periphery of the outer zone, but extends beyond it. The second region (around 80°) clearly lies outside the borders of the outer zone. In connection with the above, it would be natural to expect a difference in the character of polar aurorae in both regions. From the foregoing data on the composition of particles in the outer zone, it can be concluded that the radiation energy stored in the outer zone is sufficient for the production of polar aurorae for one week. Therefore, polar aurorae in the outer zone (55 — 65° latitude) may be due, although only partially, to the intrusion of the electrons from the outer zone into the outer part of the atmosphere. On the other hand, all polar aurorae in the polar region (about 80°) should be due directly to the intrusion of the corpuscular stream.

It can be seen from Fig. 7 that the spatial position of the outer zone on January 2, 1959 was different from that of September 12, 1959. On September 12 the maximum was observed at the distance of 17,000 km from the center of the earth, i.e., 9000 km closer to the surface of the earth than on January 2. At the same time, no difference was observed in the curves beyond the maximum. The observed large shift of the maximum possibly does not indicate a very substantial change in the spatial position of the zone, since the position of the maximum, where the zone is intersected by the rocket trajectory at large distances from the earth, is determined most probably not so much by the altitude

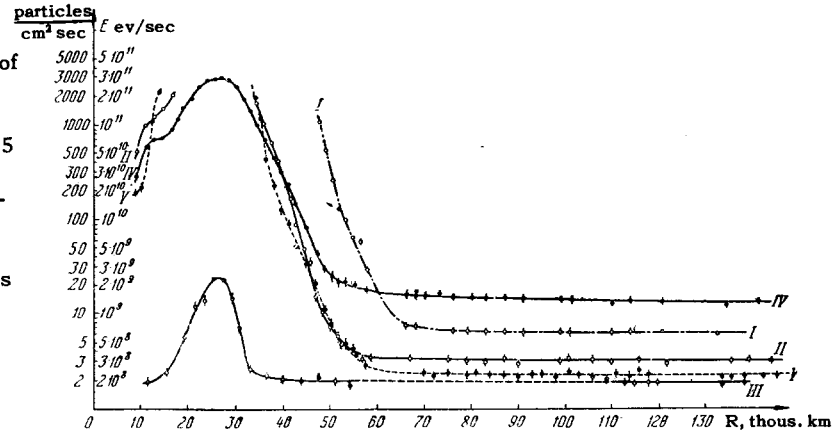

FIG. 8. Variations of the intensity with the altitude of flight of the first cosmic rocket.

R – distance from the center of the earth; I, II, III – counting rates with threshold of 45 kev, 450 kev, and 4.5 Mev respectively. The counting rate is referred to unit area of crystal cross section (19 cm²); IV – total ionization (total energy loss in the crystal per 1 sec); V – counting rate of gas-discharge counters.

The counting rate is referred to unit area of the cross section of the counters (4 and 15 cm²). The indications of both counters are in good agreement. For high intensity, the data of the smaller counters are used.

as by the intersection with a given line of force. On January 2, the maximum was observed on the line of force of 63°, and on September 12, on the line of force of 59°. Thus, it should be expected that, in the vicinity of the earth, the diameter of the zone, and possibly also its outer border, was shifted on September 12 by 4° with respect to its position of January 2. As can be seen from Figs. 5 and 6, a fluctuation of such a magnitude in the position of the borders of the outer zone is observed quite frequently. It is possible that the intensity fluctuations which are dealt with below are due mainly to this effect. Fluctuations of the position of the outer zone are evidently related to the variable character of the action of solar corpuscular streams.

S. Sh. Dolginov has drawn our attention to the fact that the flights of January 2 and September 12 differed from each other with respect to the time elapsed since the last strong magnetic storm. This period of time was much greater on January 2 than on September 12. If such a correlation is not accidental, one should assume that, after a magnetic storm, the central part of the outer zone is gradually shifted towards the peripheric region of the magnetic field.

As has already been mentioned above, it was demonstrated through the experiments carried out by means of this third Soviet earth satellite that the radiation in the outer zone consists of electrons with an average energy of about 100 kev. Data which have confirmed this conclusion, and which have also made it possible to obtain a better idea about the composition of the outer zone, were obtained by means of the first Soviet cosmic rocket. The results obtained in the flight of this rocket are shown in Fig. 8. Curves 1, 2, and 3 show the variation of the number of pulses in the scintillation counter, corresponding to an energy loss greater than 45, 450, and 4500 kev respectively, with varying distance from the center of the earth. Curve 4 shows the ionization, and curve 5 the indications of the gas-discharge counter. Along the rocket trajectory that intersected the whole outer zone, the radiation detected by all these instruments was found to represent the bremsstrahlung of the electrons absorbed in the shell of the rocket (1 g/cm² thickness). The slope of curve 3 at distances 15,000 – 35,000 km from the center of the earth can be attributed not to the detection of particles with energy higher than 5 Mev, but to the superposition of correspondingly small pulses. The shape of curve 3 strengthens this assumption, which has been fully confirmed by measurements carried out with an analogous instrument during the flight of the second cosmic rocket. For this latter flight, the resolving power of the electronic apparatus was improved by a factor of several times, and the increase of curve 3 at the maximum amounted only to about 30% of the cosmic-ray intensity.

As can be seen from Fig. 8, measurement of the number of x-ray and γ-ray quanta in the region of the radiation maximum is impossible, because their number is very large. An estimate of the photon spectrum detected by the scintillation counter can be obtained where the radiation intensity is sufficiently small, i.e., at the exit of the cosmic rocket from the outer radiation belt. At distances of 40,000 – 50,000 km from the center of the earth, we obtain

$$N(>45\text{kev}) : N(>450\text{kev}) : N(>4500\text{kev}) = 1 : 10^{-2} : 10^{-5}.$$

The data indicate that the major part of the radiation energy incident upon the crystal corresponds to x-rays with an energy of 100 kev or less. To estimate the hardness of the spectrum in the case of high-intensity radiation, we can compare the data obtained by means of the gas-discharge counter with the measurements of the total ionization in the crystal of the scintillation counter. Experiments carried out by us on the irradiation of gas-discharge and scintillation counters with x rays produced by electrons with energies in the range 20 – 100 kev have shown that the ratio K of the counting rate of the gas-discharge counter to the ionization in the crystal, i.e., to the energy flux of the x rays, increases with decreasing energy. If we compare the counting rate of the gas-discharge counter and the ionization at distances of 40,000 – 50,000 km, the ratio K corresponds to the bremsstrahlung produced by electrons with an energy of the order of 50 kev. It can be seen from Fig. 8 that the ratio K increases when approaching the maximum both from the direction of small and great distances from the earth. This means that, in the region of the maximum

of the ionization curve, the bremsstrahlung spectrum becomes softer. Estimates for distances of 1200 and 33,000 km, where the counting rate has the maximum measurable value, give an effective energy of 25 kev.

Measurements of the ionization by means of a second scintillation counter were also carried out during the flight of the first cosmic rocket. The crystal of the counter was shielded from the outer space only by an aluminum foil 1.9×10^{-3} g/cm^2 thick. Thus, it was possible to compare the energy flux under this thickness with that under a thickness of matter of 1 g/cm^2 which shielded the main scintillation counter.

It can be seen from curve 4, Fig. 8, that, at the maximum of the curve, the ionization in the crystal of the main scintillation counter amounts to 3×10^{11} ev/sec. Dividing this value by the area of the crystal and the solid angle, we find that the energy flux under a 1-g/cm^2 aluminum layer is equal to 1.5×10^9 ev cm^{-2} sec^{-1} sr^{-1}. In an analogous way, for the second scintillation counter, we find the energy flux under a thickness of 1.9×10^{-3} g/cm^2 to be equal to 2×10^{11} ev cm^{-2} sec^{-1} sr^{-1}. The ratio of the measured energy fluxes is determined by the form of the energy spectrum of the incident electrons. The second counter detected the energy flux of practically all electrons with an energy greater than 50 kev. The thickness of the crystal of the second scintillation counter was sufficiently large (0.3 g/cm^2) to ensure the measurement of the energy flux of the electrons in the range 50 — 1000 kev. The first scintillation counter measured the energy flux of x rays produced by electrons with an energy higher than 20 kev. (The threshold is determined by the absorption of x rays in the aluminum shield.)

Taking the difference in the spectral characteristics of both instruments into account, and, in particular, the variation of x-ray production efficiency as a function of the energy of incident electrons, one can draw certain conclusions concerning the energy spectrum of electrons at the outer-zone maximum.

If we assume a power-law energy spectrum $N(>E) \propto E^{-\gamma}$, then the observed ratio of the energy fluxes measured by the first and second scintillation counters leads to an estimate $\gamma \sim 5$. Such a shape of the spectrum in the energy range 20 — 100 kev is in agreement with the estimate of effective energy given above. The flux of electrons with energy greater than 20 kev can be estimated from these data as 10^9 particles cm^{-2} sec^{-1} sr^{-1}.

The analysis given above does not mean that the spectrum exponent γ remains constant in the high-energy range also. As has been shown above, the energy spectrum of photons in the range of 45 — 450 kev is relatively steep ($\gamma \sim 2$) at the border of the outer zone. This indicates the presence of electrons with an energy of the order of one or several Mev. In connection with the above, the interpretation of the observed change in the effective energy from the center of the zone to its borders can be due to one of the two following causes:

1) The average energy of the group of electrons contained in the relatively narrow range 20 — 100 kev increases. This is true if that group provides the main contribution to the ionization and to the readings of the gas-discharge counter.

2) A considerable contribution to ionization and to the indications of the gas-discharge counters is due not only to that electron group but also to electrons with energies $\gtrsim 1$ Mev. The observed variation of the effective energy can then be due to a change in the relative contribution of the second group ($E \geq 1$ Mev). The effective energy then does not represent the energy occuring most often, but is the result of averaging over two energy groups. Evidently, the second possibility is the more probable one. The presence of electrons with energies of 1 — 3 Mev has been confirmed in experiments with the second cosmic rocket by means of counters shielded by various layers of lead and copper. The flux of these electrons at the maximum amounts to $\sim 10^5$ particles cm^{-2} sec^{-1} sr^{-1}. In the energy interval $10^5 — 10^6$ ev, a high electron intensity has not been detected. The effective energy of electrons as defined above was, during the flight of the second cosmic rocket on September 12, 1959, found to be larger than during the flight of the first cosmic rocket on January 2, 1959.

Thus, we are led to the conclusion that there are two separate energy groups of electron in the outer zone: 1) the group with energies of the order of several tens of kev, and 2) the group with energies of the order of several Mev. Measurements of the hardness of the radiation inside the outer zone as a function of geographical coordinates and also of time are possibly due to the relative intensity variations of these two groups.

If we represent the energy spectrum of the first group by a power law, as has been done above, then its extrapolation to the low-energy range (5 — 10 kev) leads to the presence of a very great number of such particles. However, the number of particles trapped in a magnetic trap is limited by the condition that the energy density of these particles should be smaller than the energy density of the magnetic field $H^2/8\pi$. The energy spectrum of the first group should, therefore, be limited at the low-energy end, or, at least, the exponent of the power spectrum γ should decrease considerably for energies of the order of 10^4 ev. The first group of particles can play an essential role in the demagnetization of the magnetic field of the earth[4] and the heating of the upper layers of the atmosphere. The particle flux of the second group, consisting of electrons with energies of the order of several Mev, is considerably smaller, and this group can, therefore, hardly cause such macroscopic effects. A completely different situation prevails under an appreciable layer of matter. The first group is absorbed in comparatively thin layers of matter, and a shield of several millimeters of lead totally excludes the damaging action of this radiation. In contrast, the second group produces

γ rays having a relatively great penetrating power. Thus, for instance, γ rays of 10^6 ev are attenuated by a factor of two only by a 1 mm lead layer. Therefore, the problem of shielding from these γ rays can only be solved when their spectrum will be sufficiently well known.

Stability of the Radiation in the Outer Zone

Data on the increase of ionization during the entry of Sputnik III into the outer zone show a considerable instability of that zone. Data on the ionization increase during the entry into the outer zone in the northern hemisphere are presented in Fig. 9. In compiling these data, only those flights of Sputnik III were used in which it was possible to obtain sufficient accuracy of the ionization measurements inside and outside the zone. A systematic variation of the ionization increase with longitude has been found. This variation is due to the asymmetry of the magnetic field with respect to geographical coordinates. A corresponding correction for the longitude effect has therefore been introduced into Fig. 9. It can be seen from Fig. 9 that the number of particles in the outer zone varies sharply, sometimes by even more than an order of magnitude. Intensity variations take place during a comparatively short period of time, of the order of several hours. Attempts to find a correlation between these intensity variations and other geophysical phenomena have, so far, not given explicit results. For an illustration of this fact, the variation of the magnetic index with time is also shown in Fig. 9.

The reduced data of Sputnik III show that the intensity fluctuations are somewhat smaller in the Antarctic region. Over the Antarctic, the satellite passed at higher altitudes and fell into the intense radiation region. In contrast to this, in the northern hemisphere

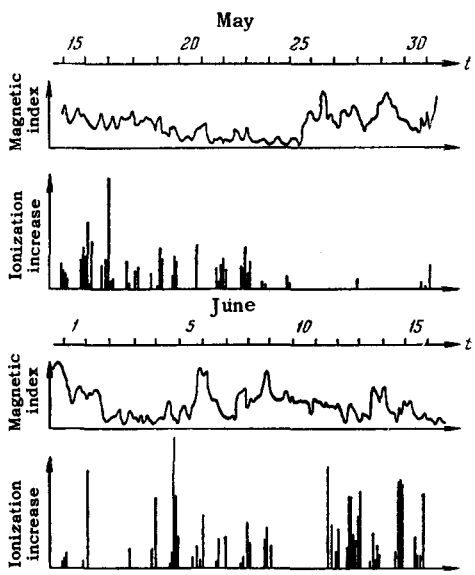

FIG. 9. The ionization effect in the outer zone over the northern hemisphere during the period from May 15 to June 17, 1958, and the world magnetic index (for a three-hour interval) during the same time.

it travelled in the outer zone only at altitudes of 400 – 500 km, i.e., near the low-altitude zone borders. It is therefore possible that the observed intensity fluctuations correspond to vertical shifts of the zone.

3. THE INNER HIGH-INTENSITY ZONE OF TCR

The first data about a high-intensity radiation in equatorial regions at altitudes greater than 1000 km were obtained by Van Allen by means of the American satellites α and γ, the trajectories of which passed in the latitude range from $+30°$ to $-30°$. The first information on the localization of the zone within a small region of space near the equator was obtained during the flight of the third Soviet satellite, the trajectory of which was contained within the latitude range $+65°$ to $-65°$. As will be shown below, the inner zone in the vicinity of the earth is observed at a geomagnetic latitude smaller than 45°. Therefore, the outer border of the inner zone could only be determined by means of a satellite whose trajectory passes through high latitudes. The trajectory of Sputnik III satisfied this condition.

Position of the Inner Zone of TCR with Respect to the Earth

Examples of the recordings carried out on board of the motor-vessel "Ob'" during the flight of Sputnik III in the region of South America are shown in Fig. 10.* The y axis represents the total energy lost in the crystal by all types of radiation. This information was obtained by measuring the dynode current. The x axis represents the geographical coordinates of Sputnik III (λ — latitude and φ — longitude). It can be seen from Fig. 10 that, in the range of geographic latitudes of $\sim 50 - 55°$, a sharp increase in the total energy release, or, what amounts to the same, of ionization in the crystal, is observed. Inside the inner zone, the energy release is greater than 10^{12} ev/sec. This value is greater by a factor of 1000 than the ionization produced in the crystal by cosmic rays. For an energy release $> 10^{12}$ ev/sec, the reading accuracy is very small. Therefore, several points in Fig. 10 are shown with arrows directed upwards. This means that the energy release is possibly several times greater than 10^{12} ev/sec. At the same time, the character of the radio signals shows that the energy release did not exceed 10^{13} ev/sec on any of the recordings.

The altitudes at which the satellite passed are shown in Fig. 10. From Fig. 10 it can be seen that, in spite of a decrease of the satellite's altitude from 1600 km to 1000 km, a strong increase in the ionization due to the entry into the inner zone is observed. This shows that the inner zone is sharply limited in the region of low geomagnetic latitudes. During the motion of the satellite from south to north (forward path),

*The authors are grateful to G. I. Golyshev and V. G. Kort for organizing these measurements.

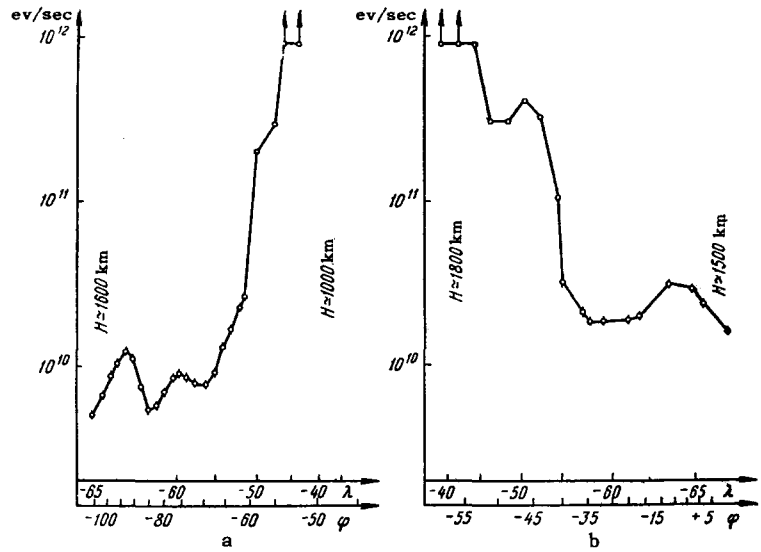

FIG. 10. Typical examples of recordings made in the region of South America.

The x axis denotes the latitude λ, longitude φ, and altitude H of the flight of Sputnik III. The y axis represents the energy released in the crystal per sec (ionization according to dynode-current measurements).

the altitude of the satellite was considerably greater than during the reverse path (motion from north to south). Therefore, a comparison of the data obtained during the forward and reverse paths in the region of South America made it possible to determine the altitude dependence of the border of the inner zone. The results of these measurements made it possible to establish that the border of the inner zone at the altitude of 1800 km lies by about 4° further to the south as compared with its position at an altitude of about 1200 km. This means that the radiation intensity increases strongly with increasing distance from the earth along a magnetic line of force. In fact, a line of force passing through a point at an altitude of 1800 km and at a latitude λ_1 will, at an altitude of 1200 km, pass through a point lying on a latitude $\lambda_2 > \lambda_1$. Therefore, if the first point lies on the outer border of the zone, then the second point certainly lies outside the zone. It should be remembered that, as has been stated above, the border of the zone at the altitude of 1200 km is located at the latitude $\lambda_3 = \lambda_1 - 4°$. Hence, $\lambda_2 > \lambda_3$. Consequently, by comparing the measurements carried out on the same magnetic line of force, we come to the conclusion that there is a strong increase in the intensity with increasing distance from the earth along a line of force. This is the experimental proof of the fact that the particles of the internal zone execute oscillations along lines of force. In other words, the inner zone, as well as the outer zone, exists because of a particle trap produced by the earth's magnetic field.

The recordings of the signals of Sputnik III near the geomagnetic equator have shown that, in the region of South America, the inner zone extends down to comparatively low altitudes, i.e., 600 km. On the other hand, the recordings of the signals of Sputnik III in Australia showed that, in that region, the lower border of the inner zone is located considerably higher, at an altitude greater than 1600 km.

Systematic data on the position of the inner zone were obtained by studying the phosphorescence of the sodium-iodide crystal. Because of the phosphorescence, our instrument possessed a certain measure of memory. The glow curve of the crystal obtained in test experiments is shown in Fig. 11. For this purpose, the crystal was irradiated for a short time by x rays, and the photomultiplier current was then measured as a function of time. It can be seen from Fig. 11 that this dependence is such that it is possible to measure the radiation dose received by the crystal during the flight of the satellite inside the inner zone. We are in possession of numerous recordings taken over the territory of the U.S.S.R., i.e., in the region between the inner and outer zones, where the intensity of the "local" radiation is sufficiently small and constant. The time elapsed between the flight of the satellite inside the inner zone and the moment of observation of phosphorescence in the crystal is about 20 — 50 min. As can be seen from Fig. 11, the phosphorescence intensity varies comparatively little in that range. Therefore, the measured value of energy loss characterizes the radiation dose during the passage of the satellite

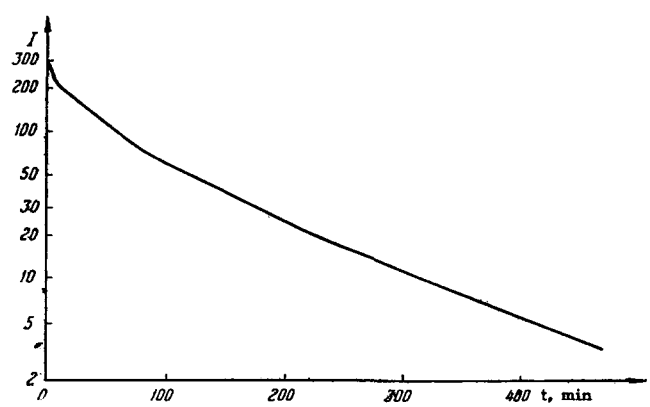

FIG. 11. Variation of the NaI crystal phosphorescence intensity with time after irradiation.

(40 min irradiation by x rays produced a crystal glow 140 times greater than the phosphorescence at t = 0.)

through the inner zone. At the same time, during the period of revolution of the satellite (about 100 min), the phosphorescence decreases sufficiently. The effect connected with the irradiation of the crystal during its previous flight through the inner zone is therefore sufficiently small. The variation of the crystal phosphorescence (lower curve, circles) with the longitude of the point of intersection of the geographical equator with the trajectory of the satellite on forward paths is shown in Fig. 12.

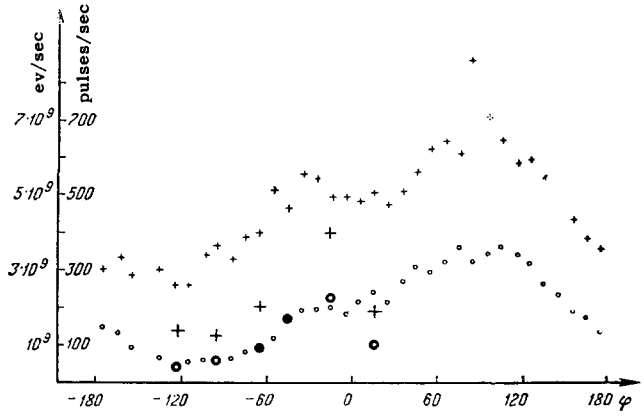

FIG. 12. Variation of the phosphorescence intensity and of the counting rate with the position of the orbit of Sputnik III with respect to geographical coordinates.

The x axis represents the latitude of the intersection of the equator for the motion of the satellite from south to north.

o – ionization outside high-intensity zones; + – counting rate with threshold 35 kev outside the high-intensity zones (data for the period from May 17 to June 7, 1958); ⊙, + – the same on May 15, 1958.

Knowing the radiation intensity in the inner zone from the direct measurements described above and from the crystal glow curve (see Fig. 11), one can estimate the absolute value of the phosphorescence intensity. Experimental data shown in Fig. 12 are in good agreement with such an estimate. The greatest value of the phosphorescence is observed at the point of intersection of the equator with longitude $\varphi = 100°$. This corresponds to a satellite trajectory passing during its reverse path through the inner zone at an altitude of 1600 km (in the region of South America). A weaker maximum is observed at $\varphi = -30°$, the longitude which corresponds to the passage of the satellite over South America during the forward path at an altitude of 800 km. The values of the two maxima differ by relatively little. This is in agreement with the conclusion reached above that, inside the inner zone, the intensity varies by less than an order of magnitude for a change of the altitude from 800 to 1600 km. Portions of the curve between the longitudes of $\varphi = -80°$ and $\varphi = -130°$ show a very small phosphorescence intensity. This means that the corresponding trajectories do not pass through the inner zone, but pass below it. Thus, we see the existence of a sharply marked longitude effect in the position of the inner zone with respect to the earth. The lower border of the zone is situated in the western hemisphere at an altitude of about 600 km and, in the eastern hemisphere, above 1600 km. This effect is due to the shift of the magnetic dipole with respect to the center of the earth in the direction of the eastern hemisphere. From the data obtained it follows that this shift amounts to not less than 500 km. Figure 13 presents the picture observed in the plane of the geomagnetic equator. The earth is represented by the shaded circle. The point shows the position of the magnetic dipole. The circle drawn with the dipole as center shows the lower limit of the inner zone. Without going into the character of the motion of charged particles in the earth's magnetic field, we note that, because of the nonhomogeneity of the earth's magnetic field, the particles drift around the magnetic dipole. The helix in Fig. 13 shows the character of the drift. The period of revolution of the particles around the earth due to the drift is very small in comparison with the period of existence of the particle in the magnetic trap. Because of that, one should expect a symmetrical distribution of particles with respect to the magnetic dipole on the magnetic equator, and the lower border of the inner zone will coincide with the circle indicated in Fig. 13.

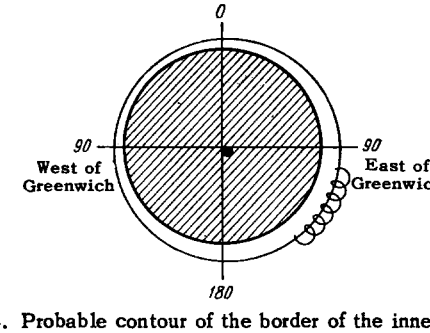

FIG. 13. Probable contour of the border of the inner zone in the plane of the geomagnetic equator. ● – center of the dipole.

The Nature and Energy of Particles in the Inner Zone

As was mentioned in the description of the apparatus, the simultaneous measurement of the anode and dynode currents of the photomultiplier made it possible to determine the energy of the particles causing the major part of the ionization in the crystal. If the energy loss in the crystal occurs in discrete amounts of less than 1 – 2 Mev, the results of ionization measurements by means of the anode and the dynode current coincide (see Fig. 4). When the energies of the single particle incident upon the crystal are large, the anode current gives values that are too low, because of saturation. Thus, for instance, when the crystal is bombarded by cosmic rays, the ionization values obtained from the anode current are smaller than the true ones by a factor of 5 – 7. In this way, a comparison of the values of the anode and dynode currents makes it possible to determine the nature of particles in the inner zone. The results of measurements carried out in America and

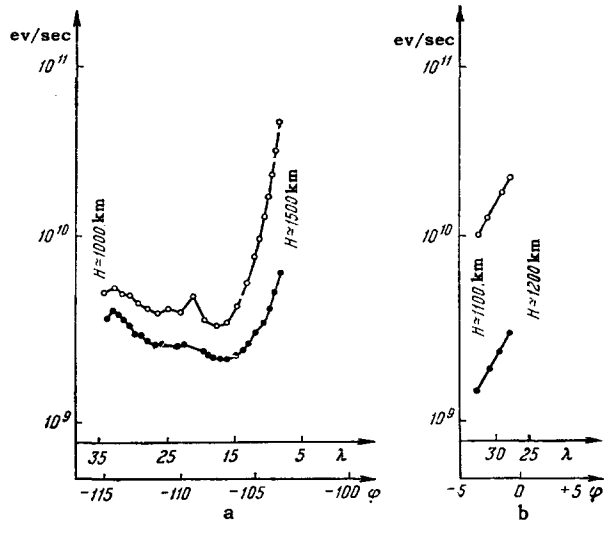

FIG. 14. Examples of recordings determining the entry of Sputnik III into the inner zone in its motion from north to south.

The x axis represents the latitude λ, longitude φ, and altitude H of the flight. The y axis represents ionization in the crystal from anode-current measurements (points) and dynode-current measurements (circles).

Africa,* and corresponding to the entry of the satellite into the inner zone, are shown in Figs. 14a and 14b. From Fig. 14a, it can be seen that the difference between the values of the anode (I_A) and dynode (I_D) currents increases with the degree of penetration into the inner zone. From Fig. 14a we find that, upon entering the zone, radiation increases so that $I_A : I_D = 1 : 8$. Figure 14b gives the results of measurements taken when the satellite was already inside the inner zone. For that case we obtain $I_A : I_D = 1 : 7$. These experimental data show that when the satellite is inside the inner zone the ionization in the crystal is due to particles with energy greater than 10 Mev. Thus, there is a difference in the composition of particles in the inner and outer zones. As has been shown above, the energy of the x-ray quanta causing the ionization is almost always less than 1 — 2 Mev and, because of that, $I_A \approx I_D$. Thus, in the inner zone, the major part of the ionization in the crystal is not caused by x rays, but directly by the charged particles that penetrate the shell of the satellite, which is ~ 1 g/cm^2 thick.

There are experimental data indicating that the high-energy particles in the inner zone are protons. The crosses in Fig. 12 indicate the number of events in which an energy greater than 35 kev was released in the crystal, measured at about 40° north geometrical latitude, i.e., in the gap between the inner and outer zones. This value is represented as a function of the longitude of the intersection of the geomagnetic equator with the trajectory of the satellite (on its forward path). The similarity of the curve obtained to the phosphorescence curve obtained earlier shows that there is also a certain amount of memory in the present case. The counting rate is, therefore, a measure of the radiation dose during the passage of the satellite through the inner zone. This can be due to the artificial radioactivity of the crystal and the surrounding material (mainly consisting of aluminum) activated by the radiation of the inner zone. The larger crosses show the data obtained on the first day of flight of Sputnik III. All large crosses fall considerably below the values obtained at the same trajectories after the lapse of many days. This shows a gradual increase in the induced radioactivity. During the period from May 20 to June 18, the counting rate for all revolutions increased by 100 counts per second. This gradual increase of the counting rate is due to the comparatively long lifetimes of the produced radioactive isotopes. The presence of the isotopes with lifetimes of the order of one hour is sufficient for memorizing the radiation dose obtained during the flight through the inner zone.

The existence of induced radioactivity is an argument for the proton nature of the particles in the inner zone. Knowing the average energy released in the crystal by the inner-zone radiation (2×10^{11} ev/sec), and estimating the value of the energy released in the crystal by radioactivity during the same time (2×10^8 ev/sec), we find that it is necessary to ascribe to particles of the inner zone the capacity of expending 10^{-3} of their energy for the production of radioactive isotopes. This would be true for protons with an energy of the order of 10^8 ev.

A hypothesis that the induced radioactivity may be due to electrons can be eliminated since, firstly, the radioactivity in that case would be weaker by several orders of magnitude, and secondly, the lifetimes would be very short.

Thus, we are led to the conclusion that protons with energy of the order of 100 Mev are present in the inner zone, and these particles cause the ionization in a crystal screened by an aluminum layer of 1 g/cm^2.

In addition to high-energy protons, low-energy particles, most probably electrons, are also present in the inner zone. The recordings of the signals of Sputnik III obtained during its approach to the inner zone in the region of America are shown in Fig. 15. In both cases, represented in Figs. 15a and 15b, we find an increase in the counting rate when the satellite was inside the outer zone (geographical latitude $\lambda > 35°$), and also an increase in the counting rate during the approach of the satellite towards the inner zone (geographical latitude $\lambda < 20°$). One should especially pay attention to the fact that, during the approach towards the inner zone, an increase in the counting rate is observed while the ionization practically does not change. This indicates the presence of low-energy particles.

Thus, the outer border of the inner zone is surrounded by a region where high-energy particles are absent while low-energy particles are present. It is most natural to explain the observed phenomenon by the presence of electrons with energies in the range 100 — 1000 kev producing bremsstrahlung in

*The measurements carried out in Africa were sent to us from England.

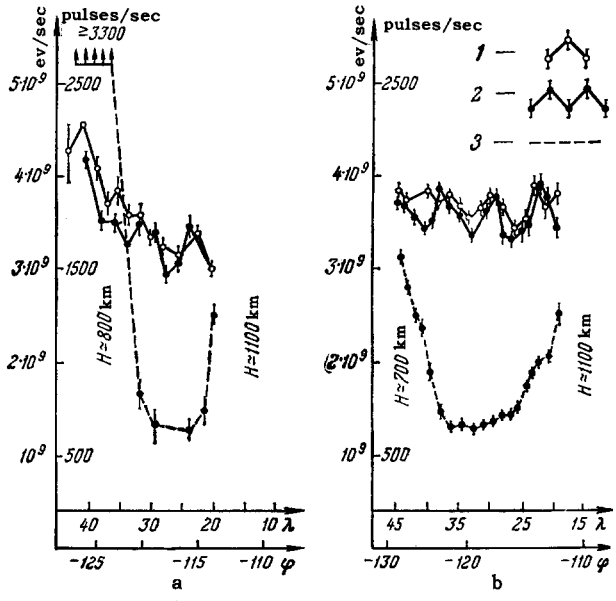

FIG. 15. Recordings indicating the exit from the outer zone and approach towards the inner zone in the northern hemisphere.

The x axis represents the latitude λ, longitude φ, and altitude H of flight of Sputnik III. 1 – counting rate; 2 – ionization in crystal from dynode-current measurements; 3 – ionization increase in crystal from anode-current measurements.

the shell of the satellite. If we want to attribute the described experimental data to low-energy protons (20 – 30 Mev) causing nuclear reactions with subsequent emission of γ rays, then, even if the particle number is recorded at an efficiency of 1%, we would have to assume a great flux of such protons. This flux would be equal to the flux of protons with E ~ 100 Mev inside the inner zone.

Consideration of Figs. 15a and 15b leads to the idea of a correlation between the variations in the inner and outer zones. From Fig. 15a we can see that the radiation of the outer zone is very intense (not only an increase in the counting rate but also an increase in the ionization is observed) and, moreover, the number of low-energy particles increases suddenly at the outer edge of the inner zone. In contrast, we can see from Fig. 15b that the outer zone has a low intensity (only an increase of the counting rate is observed, while the ionization remains constant) and, moreover, a smooth increase is observed in the number of low-energy particles at the border of the inner zone.

Stability of Radiation in the Inner Zone

The measurements of the phosphorescence over a long period provided the possibility of determining the absolute radiation intensity in the inner zone and its variation with time. The reduction of the data reveals that the radiation dose during one month remained constant within 15%. One should take into account the existence of instrumental effects which cause a variation in the sensitivity of the apparatus (temperature variations, orientation of the photomultiplier with respect to the magnetic field, etc.), and that these variations are of the same order as the observed changes of the dose. Therefore, the stability of radiation inside the inner zone can be even greater. The stability of the intensity in the inner zone indicates that particles spend a long time inside it.

4. RADIATION OUTSIDE THE EARTH'S MAGNETIC FIELD

As can be seen from Fig. 8, at distances greater than 70,000 km from the center of the earth, the intensity of radiation measured by all instruments carried by the first cosmic rocket remained constant. This means that the action of the earth's magnetic field at such distances does not change the intensity of cosmic rays. This can be due to two causes: either particles with momenta in the range $1.5 \times 10^8 - 4 \times 10^7$ ev/c are absent among cosmic rays in the interplanetary space, or, at a distance greater than 10 earth radii, the magnetic field of the earth "vanishes" (e.g., due to the existence of an interplanetary field with an intensity of 3×10^{-4} oersted).

On the second Soviet cosmic rocket launched in the direction of the moon on September 12, 1959, the gas-discharge and scintillation counters were placed not only inside the scientific apparatus container, but also outside it. The instruments placed outside the container were surrounded by a shell ~ 1 g/cm^2 thick, 20% of the total solid angle was covered by a greater amount of matter, ~ 10 g/cm^2. The instruments placed inside the container were also surrounded by a shell ~ 1 g/cm^2 thick, but the solid angle covered by thicker matter (~ 10 g/cm^2) amounted only to about 5% of the total solid angle.

The table lists data obtained during the flight of the first and second cosmic rockets. It follows from these data that the intensity of cosmic radiation consisting of high-energy particles amounts to about two particles per second per cm^2.

The value obtained is in good agreement with the measurements carried out by means of balloons in the stratosphere at high latitudes, and shows that the intensity increase in rocket experiments is due to the atmospheric albedo. From the data of the first cosmic rocket, the number of photons with energy in the range 45 – 450 kev amounts to about 3 photons sec^{-1} cm^{-2}, and in the range 450 – 4500 kev to about 1 photon sec^{-1} cm^{-2}. The measurements carried out during the flight of the second cosmic rocket give practically the same values (for measurements under analogous geometric conditions inside the container). The numbers given above represent the upper limit of the γ- and x-ray intensity in the interplanetary space. A portion of these photons may represent the secondary radiation produced by cosmic rays in the matter surrounding the instruments. The measurements carried out inside the container during the flight of the second cosmic rocket indicate that photons with energy greater than 450 kev are practically absent.

Date	Position of the apparatus	Gas discharge counter, intensity* particles/cm² sec	Scintillation counters		Ionization in NaI crystal, weighing 180 g*
			Threshold energy	Intensity‡	
2.01. 1959	Inside the container	2.3 ± 0.1	4.5 Mev 450 kev 45 kev	1.9 ± 0.1 3.0 ± 0.15 6.75 ± 0.3	(1.42 ± 0.05) × 10⁹ ev-sec
12.09. 1959	Inside the container	2.46 ± 0.1** 2.46 ± 0.1†	3.5 Mev 600 kev 60 kev	2.12 ± 0.1 2.77 ± 0.15 6.7 ± 0.3	(1.55 ± 0.05) × 10⁹ ev/sec
12.09. 1959	Outside the container	1.98 ± 0.1††	450 kev	2.02 ± 0.1	(1.15 ± 0.05) × 10⁹ ev/sec

*The errors characterize the maximum spread in the detector area.
**Counter with an additional shield of 1.5 mm Cu.
†Counter with an additional shield of 3 mm Pb.
††Counter with an additional shield of 3 mm Pb.
‡The number of pulses per second is given per unit area of the crystal (19 cm²).

It can be seen from the last row of the table that the number of particles with an energy loss greater than 450 kev is equal to 2.02 ± 0.1. At the same time, the total number of particles according to the readings of the counter placed outside the container is equal to 1.98 ± 0.1.

Thus, the number of photons which is determined from the difference of the figures given above is less than 0.1 photons cm^{-2} sec^{-1}. The ionization due to cosmic rays in the NaI crystal amounts to 1.5×10^9 ev/sec. Knowing the flux of cosmic radiation and the weight of the crystal, we found that the mean specific ionization of particles amounts to 3.5×10^6 ev g^{-1} cm^2, which is 2.5 times greater than the minimum ionization in the NaI crystal. This increased ionization can well be explained by the presence of α particles and heavier nuclei in the cosmic radiation, taking into account that a part of them are not relativistic.

5. ANALYSIS OF THE DATA OBTAINED AND POSSIBLE HYPOTHESES OF THE ORIGIN OF TCR

In order to understand the experimental results given above, it is necessary to consider briefly the motion of particles in the earth's magnetic field.

The measurements of the magnetic field at many points of the terrestrial globe have proven that, at great distances, the magnetic field can be represented by a field of a dipole tilted with respect to the earth's axis by 11.5° towards Canada. Investigations of cosmic-ray particles at various latitudes and longitudes have essentially confirmed these ideas about the earth's magnetic field. The experiments with satellites and cosmic rockets (see Secs. 2 and 3) are also in agreement with the accepted picture of the magnetic field, and have somewhat supplemented it.

The intensity of the earth's magnetic field is such that only particles with an energy considerably greater than 10^{10} ev can reach any point of the earth's surface without being markedly deflected by the earth's magnetic field. Particles of lower energies will move along strongly curved, very complicated trajectories. If the energy of the particles is sufficiently small, their motion becomes simpler. Therefore, for a sufficiently low energy, the radius of curvature of the particle trajectory in the earth's magnetic field becomes much smaller than the distance from the center of the dipole to the position of the particle. In such a case, the particles will move on helices around the lines of force of the magnetic field. If, in such motion, the particles reach the region where the magnetic field increases, a component of the magnetic field perpendicular to the axis of the helix will appear. The action of such a force will cause the particles to be reflected from the region where the magnetic field is sufficiently high. In other words, magnetic mirrors[15] are present at high latitudes.

The motion of particles is such that the magnetic moment of the particle, $\mu = mv_\perp^2/2H$, remains constant ($v_\perp$ is the component of the velocity in the direction perpendicular to the line of force, m is the mass of the particle, and H is the magnetic-field intensity). The condition that the magnetic moment be conserved will be considered below. $v_\perp = v \sin\theta$, where θ is the angle between the velocity vector and the magnetic vector at a given point of the trajectory. Hence, we have

$$\frac{2\mu}{mv^2} = \frac{\sin^2\theta}{H} = \text{const.} \qquad (1)$$

The equation of the line of force of a dipole is $R = R_e \times \cos^2\lambda$, where λ is the latitude. The magnetic field of the dipole at a given line of force characterized by R_e (Fig. 16) is equal to

$$H_\lambda = \frac{H_0\sqrt{4-3\cos^2\lambda}}{\cos^6\lambda},$$

where H_0 is the field at the point A. $H_0 = M/R_e^3$, where M is the magnetic moment of the dipole.

A particle moving at the equator at an angle θ_0 to the line of force will be reflected at point B at latitude λ_{max} given by the equation

$$\sin^2\theta_0 = \cos^6\lambda_{max}/\sqrt{4-3\cos^2\lambda_{max}}.$$

In addition to the oscillation of particles along helices around the magnetic lines of force, there will also be a rotation of the axis of the helix around the magnetic field due to the fact that the radius of curvature of the

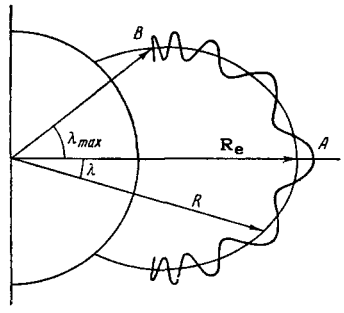

FIG. 16. Schematic representation of the motion of a charged particle along the line of force of the earth's magnetic field.

R_e – distance from the line of force to the equatorial plane; R – at a latitude λ; λ_{max} – maximum latitude which can be reached by a particle.

particle trajectory ρ increases with increasing distance from the center of the dipole. The drift velocity around the dipole is equal to

$$v_{dr} = \frac{\varrho\,[\mathrm{grad}\,H \cdot \mathrm{H}]}{2H^2}\,v_{\perp}.$$

Thus, particles of sufficiently low energy can be trapped in the magnetic trap in the vicinity of the earth. They will move inside a certain defined zone. It is clear that the only possibility of introducing the particle into the trap is to violate these equations of motion in the motion in the magnetic field, the consequences of which were discussed above.

This can be done if electrically charged particles are produced in the earth's magnetic field by neutral particles which can, without trouble, pass through the earth's magnetic field into a given point in the magnetic trap. Examples of such neutral particles are neutrons emitted from the atmosphere of the earth, or neutral atoms present in the corpuscular streams from the sun.

Another method of introducing particles into the magnetic trap is to cause a perturbation of the magnetic field for a certain period, and, in such a way, to produce a channel for the injection of particles into the magnetic trap. This can happen when dense corpuscular streams from the sun enter the magnetic field of the earth. If the energy density of the corpuscular-stream particles is higher than the energy density of the magnetic field $H^2/8\pi$, then such a bunch will disturb the magnetic field in its motion. If such a bunch is then disrupted and diffused in the magnetic trap, its particles will become trapped.

Up to now we have assumed that a charged particle moves in the magnetic field in such a way that the magnetic moment μ of the particle remains constant. However, μ is not an exact integral of the motion.[6]

It has been shown by Hellwich[7] that, if the spatial derivative of H is equal to κH, then μ remains constant at least up to the terms of the order of $(\rho\kappa)^2$. For a dipole field, κ is of the order of 1/R, where R, in our case, is almost identical with the distance to the center of the earth. Assuming that the changes of the magnetic moment can be of either sign and that they add only statistically, we find that the number of oscillations k between magnetic mirrors, i.e., from one hemisphere to the other, is equal to

$$k = \left(\frac{\mu}{\Delta\mu}\right)^2 = \left(\frac{\mu}{\left(\frac{\varrho}{R}\right)^2 \mu}\right)^2 = \left(\frac{R}{\varrho}\right)^4.$$

O. B. Firsov, using certain simplifying assumptions, showed that, before a considerable change in the magnetic moment occurs, the particles can execute a large number k of oscillations between the magnetic mirrors.

In references 9 and 10 it was shown that the number of oscillations $k = e^{\alpha R/\rho}$, where α is of the order of unity.

Thus, it has not been established yet how well the magnetic moment is conserved. One thing only is clear: for $\rho/R \ll 1$, conditions are satisfied under which the escape of particles from the magnetic trap will not be due to a change of the magnetic moment but to other reasons. As was shown by experiments carried out by means of Sputnik III (see Sec. 3), both protons with a momentum of the order of 3×10^8 ev/c and electrons with a momentum of the order of 10^6 ev/c were observed in the inner zone. Although, as is seen from Fig. 15, the low-energy particles are found at somewhat higher latitudes, the difference is still very small (on the order of 5°). If the leakage is due to the non-conservation of the magnetic moment, then the rate of escape is determined by the ratio of ρ/R. As was shown above, the momenta of particles differed by a factor of 300. Consequently, the radii of curvature ρ should differ by the same factor. The value of R is a measure of the inhomogeneities of the magnetic field. Clearly, it would be difficult to assume for any plasma oscillation that this value varies by factor of 300 for a change of latitude from 45 to 40°. Thus, there is experimental evidence supporting the assumption that the magnetic moment is conserved with such a high accuracy, that leakage from the magnetic trap (due to its nonconservation) is practically nonexistent.

We shall now consider other causes of leakage. First of all, we should consider the most simple process, i.e., the loss of the energy of the particles for the ionization of the medium.

In reference 11, we have calculated in detail the ionization losses of particles executing different oscillations, and the variation of the intensity of TCR with latitude and with the distance from the earth. The source of particle injection was assumed to be the decay, inside the magnetic trap, of the neutrons emitted by the earth's atmosphere under the action of cosmic rays.

The conditions for the injection of electrons and protons are different. In the decay of neutrons with energies in the range $10^6 - 10^9$ev, the proton conserves in practice the direction of motion of the neutron. In contrast, the electrons are emitted almost isotropically. Therefore, to calculate the intensity of the electron radiation due to neutron decay we can assume that electrons are emitted isotropically from each volume element in a quantity equal to the number

of neutrons decaying in it. In order to determine the proton intensity, it is necessary to take into account the fact that the protons are emitted from the volume element in almost the same direction as the neutron.

At great distances ($\sim 10^3 - 3 \times 10^3$ km), where the atmospheric density is very low, a particle traverses a negligibly small amount of matter ($10^{-8} - 10^{-10}$ g/cm^2) and loses on ionization an energy of $10^{-2} - 10^{-4}$ ev for each oscillation between the northern and southern mirror points. Therefore, the neutron-decay products having energies of 1 Mev and more will be able (under favorable conditions) to execute 10^8 and more oscillations. The flux intensity of these particles will increase by the same factor. It is evident that such a mechanism can lead to the appearance and constant maintenance of radiation of sufficiently high intensity around the earth, which we call "terrestrial corpuscular radiation."

We shall consider in greater detail the factors that determine the intensity of this radiation.

Let us choose an area Σ_0 in the equatorial plane, the center of which is at a distance R_e from the center of the earth. All particles with a given momentum p (for which the radius of curvature in the equatorial plane ρ_e is much less than the linear dimensions of the area Σ_0) will move inside a tube, the diameter of which at latitude λ is $\Sigma(\lambda)$.

Let the magnetic line of force passing through the point h_1, λ_1 be the axis of the chosen tube. It is clear that all particles produced in the neutron decay in different points inside this tube will traverse the diameter $\Sigma(\lambda_1)$ only under the condition that, at the point of production, the particle had such an angle θ between its velocity and the magnetic field that the equatorial plane is intercepted by its trajectory at an angle θ_0 satisfying the condition

$$\theta_{0\,\min} \leqslant \theta_0 \leqslant \theta_{\max}. \tag{2}$$

where $\theta_{0\max}$ is determined from the condition $\lambda_1 = \lambda_{\max}$. The maximum latitude $\lambda_{\max}$ which can be reached by a particle having an angle θ_0 for $\lambda = 0$ is determined from the equation

$$\frac{1}{H(\lambda_{\max})} = \frac{\sin^2\theta_0}{H(\lambda=0)},$$

i.e.,

$$\sin^2\theta_{0\max} = \frac{\cos^6\lambda_1}{\sqrt{4-3\cos^2\lambda_1}}. \tag{3a}$$

$\theta_{0\min}$ is determined from the condition $h(\lambda_{\max}) > 0$

$$\sin^2\theta_{0\,\min} = \left(\frac{R_0}{R_0+h_1}\right)^3 \frac{\cos^6\lambda_1}{\sqrt{4-3\frac{R_0}{R_0+h_1}\cos^2\lambda_1}}. \tag{3b}$$

Let $N(\theta_0, R_e, v)\,d\theta_0$ such particles be produced per second in the tube, and let these particles cut the equatorial plane in the angle interval θ_0, $\theta_0 + d\theta_0$ to the line of force and possess a given momentum p, i.e., a velocity v.

The given values of θ_0 and R_e define a corresponding trajectory with a path length $S(\theta_0, R_e)$ between two mirror points and a corresponding energy loss along this path $\Delta E(\theta_0, R_e)$. If the particle possesses an energy E_0 at its production, it can traverse the whole tube from one mirror point to the other $k(\theta_0, R_e) \sim E_0/\Delta E$ times.*

Consequently, the flux of particles per second crossing the area Σ_0 in the angle interval θ_0, $\theta_0 + d\theta_0$ will equal $k(\theta_0, R_e)\,N(\theta_0, R_e, v)\,d\theta_0$. The same particle flux crosses the area $\Sigma(\lambda_1)$ at an angle θ_1. Since the area $\Sigma(\lambda_1)$ will be crossed by all particles for which the angle θ_0 in the equatorial plane satisfies the condition (2), the total flux of particles passing through a unit sphere at latitude λ_1 is

$$j(\lambda_1, h_1) = \int_{\theta_{0\,\min}}^{\theta_{0\max}} \frac{k(\theta_0, R_e)\,N(\theta_0, R_e, v)}{\Sigma(\lambda_1)\cos\theta_1}\,d\theta_0;$$

However, $\Sigma(\lambda_1)\,H(\lambda_1) = \Sigma_0 H_0$; thus, $\Sigma(\lambda_1) = \Sigma_0 H_0 / H(\lambda_1) = \Sigma_0 \cos^6\lambda_1/\sqrt{4-3\cos^2\lambda_1}$. We shall denote by $n(\theta_0, R_e, v) = N(\theta_0, R_e, v)/\Sigma_0$ the number of particles per second produced in the whole tube that passes through the observation point and has a cross section area of 1 cm^2 at the equator. Finally, we obtain the following expression for $j(\lambda_1, h_1)$

$$j(\lambda_1, h_1) = \frac{\sqrt{4-3\cos^2\lambda_1}}{\cos^6\lambda_1} \int_{\theta_{0\,\min}}^{\theta_{0\max}} \frac{n(\theta_0, R_e, v)\,k(\theta_0, R_e)}{\cos\theta_1\,(\theta_0, \lambda_1)}\,d\theta_0. \tag{4}$$

Here

$$\cos\theta_1 = \sqrt{\frac{\cos^6\lambda_1 - \sin^2\theta_0\sqrt{4-3\cos^2\lambda_1}}{\cos^3\lambda_1}},$$

$$\sin^2\theta_{0\max} = \frac{\cos^6\lambda_1}{\sqrt{4-3\cos^2\lambda_1}};\quad \sin^2\theta_{0\,\min} = \frac{\left(\frac{R_0}{R_0+h_1}\right)^3\cos^6\lambda_1}{\sqrt{4-3\frac{R_0}{R_0+h_1}\cos^2\lambda_1}}.$$

As can be seen from Eq. (4), the value of the observed flux is determined essentially by two quantities: the storage factor $k(\theta_0, R_e)$ proportional to the lifetime of particles, and the quantity $n(\theta_0, R_e, v)\,d\theta_0$,

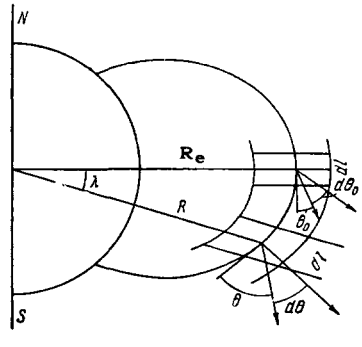

FIG. 17. Pertaining to the calculation of the number of particles produced per second in a tube of 1 cm^2 cross section at the equator.

which depends on the production conditions of particles in the neutron decay. We shall calculate the number of particles per second produced in a tube with 1 cm^2 cross section at the equator (Fig. 17).

*Since ionization losses depend on the particle energy, the accurate value of ΔE should be expressed in terms of the range of particles (see below).

Let us consider a volume element of the tube at a latitude λ and equal to $dV = \sigma dl$, where σ is the cross section of the tube, $\sigma = \cos^6\lambda/\sqrt{4-3\cos^2\lambda}$, and dl is the element of length of the magnetic line of force. If the neutron flux incident upon the volume element dV is equal to n_n, then $n_n \sigma dl/\tau_0 v_n$ neutrons decay each second in this volume. From all the decay products in the volume element, it is necessary to select only those having angles in the interval θ_1, $\theta_1+d\theta_1$, such that these particles will have angles in the interval θ_0, $\theta_0+d\theta_0$ at the equator.

As far as electrons are concerned, these are emitted isotropically in the neutron decay, and the number of decay electrons having angles in the interval θ_1, $\theta_1+d\theta_1$ is therefore equal to

$$\frac{n_n(\lambda, R_e, v)\cos^6\lambda \frac{d\theta_1}{d\theta_0}\sin\theta_1 d\theta_0 dl}{\tau_0 v_n \sqrt{4-3\cos^2\lambda}}. \quad (5)$$

The total number of decay electrons produced in the whole tube is given by the equation

$$n_e(\theta_0, R_e, v)d\theta_0 = \frac{d\theta_0}{\tau_0 v_n}\int_0^{\lambda_{max}} n_n(\lambda, R_e, v)\frac{\cos^6\lambda}{\sqrt{4-3\cos^2\lambda}}\sin\theta_1\frac{d\theta_1}{d\theta_0}dl.$$

Since $dl = R_e\cos\lambda\sqrt{4-3\cos^2\lambda}\,d\lambda$, $\sin\theta_1 = \sin\theta_0 \times (4-3\cos^2\lambda)^{1/4}/\cos^3\lambda$ and $d\theta_1/d\theta_0 = \cos\theta_0 \times\sqrt{4-3\cos^2\lambda}/\sqrt{\cos^6\lambda - \sin^2\theta_0\sqrt{4-3\cos^2\lambda}}$, we finally obtain

$$n_e(\theta_0, R_e, v)d\theta_0 = R_e\frac{\cos\theta_0\sin\theta_0 d\theta_0}{\tau_0 v_n} \times\int_0^{\lambda_{max}}\frac{n_n(\lambda, R_e, v)\cos^4\lambda(4-3\cos^2\lambda)^{\frac{1}{2}}}{\sqrt{\cos^6\lambda-\sin^2\theta_0\sqrt{4-3\cos^2\lambda}}}d\lambda, \quad (6)$$

where λ_{max} satisfies Eq. (3a), and $n_n(\lambda, R_e, v)$ is the neutron flux through a unit sphere at a latitude λ on the magnetic line of force passing through the equator at the distance R_e from the center of the earth.

In connection with the fact that protons in practice conserve the direction of motion of the parent neutrons, the number of protons produced in the volume dV in the angle range θ_1, $\theta_1+d\theta_1$ is given by the equation

$$n_p(\lambda, R_e, \theta_1)d\theta_1 = n_n(\lambda, R_e, \theta_1)d\theta_1\frac{\sigma dl}{\tau_0 v_n}.$$

Similarly to the case of electrons, the total number of protons in the whole tube is given by the formula

$$n_p(\theta_0, R_e, v)d\theta_0 = \frac{R_e\cos\theta_0 d\theta_0}{\tau_0 v_n}\int_0^{\lambda_{max}}\frac{n_n(\lambda, R_e, \theta_1, v)\cos^7\lambda(4-3\cos^2\lambda)^{\frac{1}{4}}}{\sqrt{\cos^6\lambda-\sin^2\theta_0\sqrt{4-3\cos^2\lambda}}}d\lambda, \quad (7)$$

where $n_n(\lambda, R_e, \theta_1, v)$ is the flux of neutrons travelling at the angle θ_1 to the vector H through a unit sphere at latitude λ and at a distance $R = R_e\cos^2\lambda$ from the center of the earth.

Thus, in order to calculate finally the injection of electrons and protons, i.e., to obtain the value giving the angular distribution of charged particles in the equatorial plane at a given distance R_e from the center of the earth, it is necessary to calculate the neutron flux $n_n(\lambda, R_e, \theta_1, v)$. Point 1 (Fig. 18) will be reached at an angle θ by neutrons leaving the earth's atmosphere along the generators of the circular cone (with an aperture angle θ and direction of axis coinciding with the direction of the magnetic field H at point 1), and which are emitted from the part of the curve along which the cone intersects the surface of the earth that is visible from point 1.* We shall consider two coordinate systems: (x, y, z) or $(R, \pi/2-\lambda, \varphi)$ with its origin at point O, and (x', y', z') or (d, ϑ, ψ) with its origin at point 1 having coordinates $(R, \pi/2-\lambda, 0)$. The system (x', y', z') is rotated with respect to (x, y, z) by the angle $\gamma = \pi/2-\lambda+\alpha$ in the plane yz. Let us consider a certain unit area at point 1. From point 1, we can see on the sphere an area (around point 2) subtending an angle $d\omega$

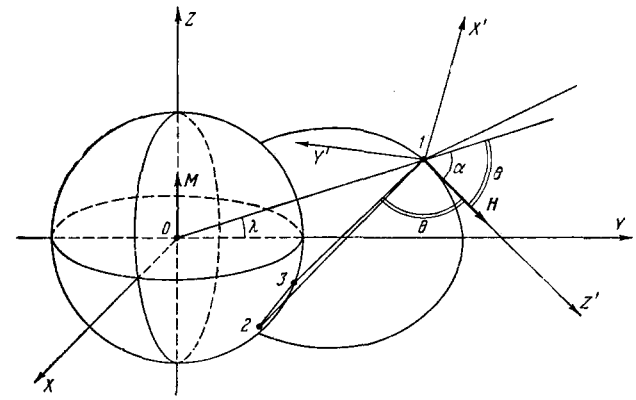

FIG. 18. Pertaining to the calculation of the injection of particles into point 1 on a given line of force.

$$d\sigma = \frac{\sin\vartheta\, d\vartheta\, d\psi\, d^2}{\cos\xi},$$

where ξ is the angle between the radius of the earth passing through point 2 and the generator of the cone, and d is the distance between the points 1 and 2. From point 2, we see the area $d\sigma_{vis} = \cos\vartheta$. This area is traversed by $I(\xi, \lambda)d\sigma(1/d^2)d\sigma'_{vis}$ neutrons emerging from $d\sigma$. $I(\xi, \lambda)$ denotes the function for the number of neutrons emitted through the horizontal unit area at latitude λ at an angle ξ to the normal to this area per unit solid angle. The total number of neutrons per unit solid angle coming from the whole surface of the earth and traversing a unit sphere at point 1 at an angle ξ is then given by the equation

$$f(\lambda, \theta, R_e) = \frac{1}{\psi_2-\psi_1}\int_{\psi_1}^{\psi_2}\frac{I(\xi, \lambda)}{\cos\xi}d\psi. \quad (8)$$

*More accurately, one should not talk about the surface of the earth, but about the surface of a sphere within which, to a degree of accuracy necessary for the present problem, practically the whole atmosphere is contained. The angular and energy distributions of the neutrons emitted by the atmosphere should be given at this surface.

The neutron flux flowing at an angle θ to the vector **H** through a unit sphere is given by the equation

$$n_n(\lambda, R_e, \theta) = f(\lambda, \theta, R_e) \sin\vartheta\, d\vartheta\, (\psi_2 - \psi_1).$$

Integral (8) can be calculated by expressing ξ and λ in terms of the variables d, ϑ, and ψ. The limits of integration can be determined in the following way: It is not difficult to see from Fig. 18 that ψ_2 always equals $\pi/2$. In the coordinate system (d, ϑ, ψ), we can write the expression for the distance d from point 1 to the point of intersection between the generator of the cone with the surface of the earth

$$d = -Rb \pm \sqrt{(Rb)^2 - (R^2 - R_e^2)}, \qquad (9)$$

where $b = -\sin\psi \sin\vartheta \sin\alpha + \cos\vartheta \cos\alpha$. It is easy to see that the generatrix of the cone, making an angle ψ_1, is tangent to the surface of the earth. Therefore, for a given R_e and ϑ, the angle ψ_1 can be determined from the condition

$$(Rb)^2 - (R^2 - R_e^2) = 0. \qquad (10)$$

If Eq. (10) has no solution, then this means that $\psi_1 = -\pi/2$, as can easily be seen.

Thus, to calculate the injection it is necessary to know the function $I(\xi, \lambda)$. If we are interested in fast neutrons only, this function can be calculated approximately in the following way, as was shown by I. P. Ivanenko and V. S. Murzin: Let us consider the production of a reverse neutron flux due to scattering of the neutrons produced in stars. These neutrons can be divided into three groups:

1. Low-energy evaporation neutrons. These have an isotropic angular distribution. Their energy distribution is Maxwellian, with an average energy of ~ 10 Mev. The multiplicity per disintegration of a light nucleus has been determined in reference 12, and is equal to $n \sim 3.5$.

2. The second group consists of δ neutrons of energy $E \gtrsim 50$ Mev. It is rather difficult to observe these experimentally. It is, however, reasonable to assume that their multiplicity and angular and energy characteristics differ little from the corresponding characteristics of protons of the same energies produced in the same stars. For 50 — 100 Mev protons, it was found[13] that they are emitted only in the forward hemisphere, and that their angular distribution is best approximated by the expression $f(\psi) \propto \cos^3\psi$, where ψ is the angle between the direction of motion of the neutrons and of the primary particle. According to estimates,[13] ~ 0.5 neutron with $E \gtrsim 50$ Mev is produced in a single interaction. The spectrum is $dN/dE \propto E^{-3}$.

3. The third group consists of neutrons of intermediate energies, 25 Mev $\lesssim E \lesssim$ 50 Mev. It is reasonable to assume that such neutrons have an intermediate angular distribution $f(\psi) \propto \cos\psi$. We shall assume that the energy spectrum in this range is identical to the spectrum in the energy range $E \gtrsim 50$ Mev. Their number will then be equal to ~ 0.5 per star.

It should be noted that the neutrons of the second group are produced in high-energy stars (excitation energy $\sim 0.5 - 1$ Bev), and those of the first group in low-energy stars. The producing components of the two neutron groups will therefore have a different altitude dependence. For the second group, this will be given by an exponential function with an exponent of ~ 120 g/cm^2. For the first group, the altitude dependence has a maximum, and is given by the expression[13]

$$I(x, \theta) = I_0 e^{-\frac{x}{L\cos\theta}} \sum_{n=0}^{3} \left(\frac{x}{n!\, L\cos\theta}\right)^n \quad \text{for } x < 300 \text{ g/cm}^2$$

where L is the nucleon mean free path, and θ is the zenith angle. Taking into account only the production of neutrons in stars and their absorption during their motion back towards the top of the atmosphere (we assume that $L_p = 2Lb_3 = 120$ g/cm^2), we can obtain the angular distribution for all three neutron groups at the top of the atmosphere. In the calculations, it was assumed, in accordance with reference 14, that a flux of primary protons through a unit sphere at a fixed altitude at a given latitude λ is proportional to $\cos^{-5}\lambda$ for $0° \leq \lambda \leq 50°$. The numerical results obtained can be approximated sufficiently accurately by the following analytical expressions:*

1. For the first neutron group:

a) produced in stars by high-energy protons

$$I(\xi) = \frac{1}{3}\left(1 + \frac{16}{3}\frac{\cos^4\xi}{(1+\cos\xi)^3}\right);$$

b) produced in stars by low-energy neutrons

$$I(\xi) = 1 - \cos\xi \ln\left(1 + \frac{1}{\cos\xi}\right).$$

2. For neutrons of the second group:

$$I(\xi) = 2.2e^{-3\cos\xi - \frac{1.4}{\cos\xi}} \exp\left(-\frac{(\cos\xi - \cos 45°)^2}{0.072}\right),$$

3. For neutrons of the third group:

$$I(\xi) = 16.7e^{-5\cos\xi - \frac{0.3}{\cos\xi}} \exp\left(-\frac{(\cos\xi - \cos 45°)^2}{0.09}\right).$$

In order to determine the flux of particles of the "terrestrial corpuscular radiation," it is necessary to know the "storage factor" $k(\theta_0, R_e)$. In the case where the ionization loss represents the main reason for the energy loss, $k(\theta_0, R_e) = Z_0/\Delta x(\theta_0, R_e)$. Z_0 denotes here the range corresponding to the energy E_0, and Δx is the amount of matter traversed by the particle between two mirror points. There is a basis for assuming that, in the passage of the particles through the atmosphere, the total losses, including the losses in collisions of the particles both with atomic electrons and with electrons of the plasma, are roughly equal to ionization losses. Therefore, for the calculation of the radiation intensity, it is necessary to know the

*In all expressions for $I(\xi, \lambda)$ given below, we neglect the dependence of this function on λ (which enters as a separate factor), and show only the dependence $I(\xi)$.

density at the altitudes greater than 300 km, up to those distances from the earth which are reached by the particles in their oscillations inside the magnetic trap. As we have seen above, this limit amounts to 10 earth radii for the outer zone, and to ~ 1 radius of the earth for the inner zone. The atmosphere density has, at present, been measured up to the altitude of ~ 400 km.[15] At greater altitudes, the density was estimated on the basis of the data on the number of electrons and ions by means of the theoretical considerations on the degree of ionization in the atmosphere.[16] In the distance range 400 — 1000 km, these estimates yield for the most part only the order of magnitude. It is difficult to take into account the degree of ionization of the atmosphere, i.e., the ratio of the number of charged particles to the total number of atoms. At altitudes above 600 km, Singer, assuming that above this level the particles move without collisions, calculated the altitude density variation assuming only a given temperature of those atmospheric layers from which the particles are emitted. Singer found that, for a motion of the neutral atoms in the gravitational field of the earth, and for a Maxwellian distribution of their velocities below the exosphere, a standard velocity distribution should be established inside the exosphere. This is due to the fact that the decrease in the energy of atoms as they recede from the center of gravitation, i.e., in the given case from the earth, is automatically compensated for by the overwhelming presence, at high altitudes, of atoms having a high energy when leaving the atmosphere. This enabled Singer to carry out a quantitative calculation of the density at very high altitudes. However, as was observed by A. I. Lebedev and I. P. Ivanenko, the motion of the particle will be determined at high altitudes not only by the gravitational forces but by Lorenz forces as well, because of practically total ionization of the atmosphere. As a result, a definite density distribution along magnetic lines of force will be established. In other words, the density will depend not only on altitude, but also in a definite manner on geomagnetic latitudes and longitudes.

The above considerations show that it is difficult, at present, to make a choice between the various models of the atmosphere, and to obtain the necessary data for the calculation of the variation of density with altitude. It seems to us that the reverse procedure should be possible, i.e., to calculate the intensity of proton and electron radiation for different models of the atmosphere, based on the data on neutrons emitted from the atmosphere, and to compare these calculations with the experimental data on TCR given above.

Exact calculations will be published in the future. In the present article, we shall carry out only a qualitative comparison.

Protons with energy of the order of 10^8 ev, found by us to be present in the inner zone, can obviously only be produced by cosmic-ray neutrons, as it is difficult to imagine any other mechanism of their origin. We shall therefore concentrate our attention on the proton component of the inner zone. The sharp borders of this zone (see Fig. 10), enclosing a part of space adjacent to the earth, cannot be explained by any reasonable assumptions on the variation of the density with altitude, longitude, and latitude. There is no doubt that, on the lines of force of 40° latitude,* the leakage from the trap becomes very great. At the same time, on magnetic lines of force with latitudes smaller than 30°, the leakage should be so small that the lifetime of a proton would amount to about 100 days.

As was shown in Sec. 3, the intensity varies relatively little in the inner zone. This can be considered as an experimental indication of the existence of two types of leakage: 1) almost independent of latitude, and 2) sharply increasing on lines of force with latitude greater than 35°, and practically negligible for lower latitudes.

The leakage of the first type is apparently due to ionization losses, since the experimental data might agree with the hypothesis about the decay of cosmic-radiation neutrons, under reasonable assumptions concerning the altitude variation of the density. The sharply-defined low-altitude border of the inner zone at the equator (600 km for the western hemisphere) finds its natural explanation in the fact that the atmospheric density is sufficiently great below this altitude. The estimates carried out showed that there is a possibility for a quantitative agreement between theory and experiment.

In the present article, we shall not dwell upon a discussion of the magnetic bremsstrahlung losses and of losses due to Coulomb scattering. These can be fully neglected for protons. For electrons produced in neutron decay, these losses, although not negligibly small, cannot change the order-of-magnitude estimates carried out taking only ionization losses into account. The presence of scattering can lead not so much to the loss of particles as to a change of the dependence of their number on the angle θ to the line of force. If, in addition to Coulomb scattering, there exists an additional stronger scattering by inhomogeneities in the plasma inside the magnetic trap, then a marked effect can also exist for protons in that case.

Let us now consider leakage of the second type. We also can ask whether the two experimental facts, the existence of the outer zone and the limitation of the inner zone, are not due to the same cause.

It is possible that the violation of the laws of motion of charged particles in a stationary magnetic field leads to the leakage of particles from the inner zone. At the same time, the same reasons may lead to the penetration of particles into the region of the outer zone, and thus to its creation. The clear difference between the composition of particles in the inner and outer zones then becomes understood. The gap between the zones should then be regarded as such a

*Here, as before, we designate a magnetic line of force by the latitude at which it intersects the surface of the earth.

region of the space where, on the one hand, the leakage is sufficiently great (lifetime less than 10^4 sec), but on the other hand the leakage is not sufficient to let a large number of particles from the interplanetary space through.

It should be noted that this point of view is not the only possible one, mainly because of two reasons:

1) The processes may be irreversible. For instance, as mentioned in the beginning of the article, plasma bunches may fall inside the outer zone and then diffuse. A reversible process, i.e., the production of a moving bunch and its ejection from the magnetic trap, is extremely improbable from statistical considerations.

2) The leakage of the particles may lead to the translation of the particles not along the radius but along the lines of force. In other words, the leakage may be due to the fact that the altitude of particle oscillations along lines of force will increase, and the particle will reach the denser atmospheric layer.

A specific mechanism by which the variable component of the magnetic field may influence the lifetime of a particle consists in the increase of the particle energy in collisions with magnetic stoppers oscillating in space. These oscillations of the reflection points should have the same frequency as the field and an amplitude of the order of $a = R(\delta H/H)$, where $\delta H/H$ is the relative variation of the magnetic field. The particles will be accelerated with conservation of the magnetic moment, essentially in analogy will the Fermi statistical acceleration mechanism. The energy gain per collision amounts to:

$$\delta E \sim \frac{mc^2}{\sqrt{1-\beta^2}} B^2 = \frac{mc^2}{\sqrt{1-\beta^2}} \left(\frac{\omega R}{c}\frac{\delta H}{H}\right)^2,$$

where $B = u/c$ and u is the velocity of motion of the magnetic stopper. Since the magnetic moment is conserved, a considerable increase in the kinetic energy of the particle will produce a corresponding increase in the amplitude of oscillations along the line of force and the particle will be absorbed in the atmosphere. For relativistic particles ($n \leq 10^8$) we obtain $\omega(\delta H/H) \sim 3 \times 10^{-3}$, i.e., for $\delta H/H = 1\%$, for example, the period of field oscillations should be $\lesssim 20$ sec.

Such a mechanism ensures an electron leakage only several times weaker than that for protons. In this connection, one should expect a similarity in the spatial distribution of the particles of both kinds in the inner zone. The electrons should have a somewhat wider distribution (since their velocity is closer to the velocity of light). The available experimental data favor such a picture.

It should be noted that this neutron mechanism of corpuscular radiation in the vicinity of the earth is responsible primarily for the creation of the inner zone.

The corpuscular stream emitted by the sun may be the source of particles injected into the outer zone. The electrons appearing in the outer zone may be transported from the sun in magnetic traps. An indication of the existence of such traps was obtained in our stratospheric experiments.[17]

Another possible mechanism is the energy transfer from the protons to the electrons in collisions of the corpuscular stream with the magnetic field of the earth, or during their long stay in the earth's magnetic field.

We can suggest the following possible way of injection of protons of energy of $10^4 - 10^5$ ev into the outer zone. The corpuscular streams from the sun contain neutral atoms that amount to approximately 1% of the total number of particles. Some of these atoms are ionized inside the outer zone and are consequently caught in the magnetic trap. The ionization is due to ultra-violet rays of the sun and to particles present in the outer zone.

Such a mechanism naturally leads to the injection of protons rather than electrons. Yet, electrons were discovered experimentally in the outer zone. This mechanism can therefore play an important role if it is possible to transfer energy from the protons to the electrons, at least during the long stay of these particles in the trap.

This mechanism whereby radiation is produced by decay of neutrons, discussed in detail above, should undoubtedly occur near astrophysical objects possessing a magnetic field. For other mechanisms, one cannot draw such definite conclusions, since the properties of the interplanetary space (for instance, the character of corpuscular streams) may depend on the distance from the sun. However, with certain modifications, other mechanisms can also produce radiation belts around celestial bodies. The existence of such radiation in the vicinity of the planets of the solar system can therefore serve as a means for detecting even weak magnetic fields. Calculations show that, in such a way, one can detect a magnetic moment one-thousandth that of the earth.

During the flight of the second Soviet rocket to the moon it was established that there are no radiation belts around the moon. At distances greater than 1000 km from the moon, the intensity of additional radiation is less than 10^{-6} of the intensity of the same radiation in the outer zone of TCR. At altitudes of $0 - 1000$ km (over the moon) the corresponding ratio is less than 10^{-4}. We can thus conclude that there is practically no lunar corpuscular radiation.

CONCLUSIONS

1. Two zones of high-intensity radiation, separated from each other, exist around the earth.

2. The outer zone begins in the equatorial plane at a distance of about 20,000 km from the center of the earth, and spreads outward up to distances of about 60,000 km. The borders of the zone are formed by the lines of force of the geomagnetic field. At relatively low altitudes ($300 - 1500$ km), the outer zone is observed at geomagnetic latitudes from 55 to 70°. With increasing distance from the earth along the lines

of force, a sharp increase of the radiation intensity is observed, which provides the experimental proof of the existence of a magnetic particle trap around the earth. Considerable time variations of the radiation intensity in the outer zone have been recorded. During the flight of the first Soviet cosmic rocket on January 2, 1959, the radiation maximum was found at 26,000 km from the center of the earth at the line of force intersecting the surface of the earth at 63° latitude. During the flight of the second Soviet cosmic rocket on September 12, 1959, the maximum was found at 17,000 km at the 59° line of force.

3. The outer zone is composed of electrons. Two separate energy groups are present. The first group consists of electrons with energy of the order of several times ten kev. The flux of electrons with energy greater than 20 kev at the maximum amounts to 10^9 cm^{-2} sec^{-1} sr^{-1}. The second group consists of electrons with energy of the order of 10^6 ev. The flux of such electrons at the maximum amounts to 10^5 cm^{-2} sec^{-1} sr^{-1}.

4. The inner zone begins in the equatorial plane at an altitude of 600 km in the western hemisphere and spreads to a distance of the order of one earth radius. The inner zone is bounded by the line of force intersecting the surface of the earth at 35° geomagnetic latitude. The radiation intensity in the inner zone remained constant for about one month, at least within 15%.

5. The inner zone is composed of protons with energy of about 10^8 ev. The flux amounts to 10^2 protons $cm^{-2}sec^{-1}$ sr^{-1}. At the borders of the inner zone, roughly in the region of $35 - 40°$ geomagnetic latitude, low-energy radiation (less than 10^6 ev) is observed, evidently consisting of electrons. It is natural to suppose that this radiation is also present throughout the inner zone.

6. Between the two zones, in the range of geomagnetic latitudes of $40 - 55°$, a region is observed where increased radiation intensity is practically absent. Basing ourselves on the accuracy of the measurements, it is possible to maintain that the flux of electrons with energy greater than 100 kev in that region at an altitude of $300 - 700$ km is less than 10^{-3} of the same flux inside the outer zone. The flux of protons with energies above 10^8 ev is less than 10^{-3} of the same flux inside the inner zone.

7. Outside the magnetic field of the earth, the radiation consists of protons and other nuclei. The total flux amounts to 2 particles-cm^{-2}-sec^{-1}. The mean specific ionization of high-energy charged particles is greater than the minimum ionization by a factor of 2.5. The flux of photons in the interplanetary space with an energy $h\nu > 450$ kev is less than 0.1 photon-cm^{-2}-sec^{-1}, and, with energy $h\nu > 45$ kev, it is less than 3 photons-cm^{-2}-sec^{-1}. Thus, hard electromagnetic radiation does not play a great role in cosmic space.

During the flight of the first and second cosmic rockets, no variations of the above radiation components greater than a few percent (for an averaging time of $10 - 20$ min) were observed.

8. Comparison of experimental data with theoretical considerations shows that high-energy protons in the inner zone may be due to the decay of neutrons emitted by the atmosphere of the earth. The radiation intensity at the center of the inner zone at small altitudes is determined by the ionization losses of protons in the upper layers of the atmosphere. At geomagnetic latitudes greater than 30°, and correspondingly at higher latitudes in the equatorial plane, the intensity begins to fall off sharply due to the inadequacy of the magnetic trap at these latitudes. This inadequacy of the magnetic trap appears almost the same both for high-energy and low-energy particles (see point 5 of the conclusions). It is therefore not very probable that the inadequacy of the magnetic trap is connected with the non-conservation of the magnetic moment of the particles.

[1] Vernov, Grigorov, Logachev, and Chudakov, Dokl. Akad. Nauk SSSR **120**, No. 6 (1958), Soviet Phys.-Doklady **3**, 617 (1959).

[2] S. N. Vernov and A. E. Chudakov, Investigation of Cosmic Rays by Means of Rockets and Satellites in the U.S.S.R., Paper presented at the 5th IGY Assembly 1958; A. E. Chudakov, Investigation of Photons by Means of Sputnik III. Paper presented at the 5th IGY Assembly 1958; S. N. Vernov and A. E. Chudakov, Investigation of Cosmic Rays by Means of Rockets and Satellites in the U.S.S.R. Paper presented at the Second International Conference on Peaceful Applications of Atomic Energy; Vernov, Chudakov, Vakulov, Gorchakov, and Logachev, "Искусственные спутники Земли" (Artificial Earth Satellites), No. 2, 1958; Vernov, Chudakov, Gorchakov, Logachev, and Vakulov, Planet. Space Sci. **1**, 86 (1959).

[3] Vernov, Chudakov, Vakulov, and Logachev, Dokl. Akad. Nauk SSSR **125**, No. 2 (1959), Soviet Phys.-Doklady **4**, 338 (1959). S. N. Vernov and A. E. Chudakov, Paper presented at the International Cosmic-Ray Conference, 1959.

[4] S. Sh. Dolginov and N. V. Pushkov, Paper presented at the International Cosmic-Ray Conference, 1959.

[5] G. I. Budker, Физика плазмы и проблема управляемых термоядерных реакций (Plasma Physics and the Problem of Controlled Thermonuclear Reactions), Academy of Sciences U.S.S.R., 1958, Vol. III, p. 3.

[6] N. N. Bogolyubov and Yu. A. Mitropol'skiĭ, Асимптотические методы в теории нелинейных колебаний (Asymptotic Methods in the Theory of Nonlinear Vibrations), Moscow, 1959.

[7] Hellwich, Z. Naturforsch. **10a**, 508 (1955).

[8] O. B. Firsov, loc. cit. ref. 5.

[9] R. M. Kulsrud, Phys. Rev. **106**, 205 (1957).

[10] F. Herfweek and U. A. Schlüter, Z. Naturforsch. **12a**, 844 (1957).

[11] Vernov, Grigorov, Ivanenko, Lebedinskiĭ, Murzin,

and Chudakov, Dokl. Akad. Nauk SSSR **124**, 1022 (1959), Soviet Phys.-Doklady **4**, 154 (1959).

[12] J. Wilson, editor, Progress in Cosmic-Ray Physics (North Holland Publishing Co., Amsterdam, 1952), Vol. I (Russ. Transl. IIL, 1954, p. 263).

[13] V. S. Murzin, Dissertation, Moscow 1955.

[14] Vernov, Kulikov, and Charakhch'yan, Izv. Akad. Nauk SSSR, Ser. Fiz. **17**, 3 (1953).

[15] V. Mikhnevich, "Искусственные спутники Земли" (Artificial Earth Satellites), No. 2. Article by the President of the Academy of Sciences U.S.S.R., "Pravda."

[16] Ya. L. Al'pert et al., Usp. Fiz. Nauk **65**, 161 (1958).

[17] A. N. Charakhch'yan, Paper presented at the International Cosmic-Ray Conference, 1959.

See also the paper of J. A. Van Allen, in which references to the papers of Van Allen are given.

Translated by H. Kasha